Editors' choice

The oldest shark face—anatomy of the Devonian elasmobranch *Phoebodus*

CHRISTIAN KLUG, MERLE GREIF, ALEXANDER POHLE, MICHAŁ GINTER, MICHAEL I. COATES, WAHIBA BEL HAOUZ, ABDELOUAHED LAGNAOUI, JONATHAN POPLE, and LINDA FREY

Klug, C., Greif, M., Pohle, A., Ginter, M., Coates, M.I., Bel Haouz, W., Lagnaoui, A., Pople J., and Frey, L. 2026. The oldest shark face—anatomy of the Devonian elasmobranch *Phoebodus*. *Acta Palaeontologica Polonica* 71 (2): 399–430.

Phoebodus was recognized as the earliest elasmobranch known from articulated remains, a group which constitutes most modern cartilaginous fish comprising sharks, skates and rays. Its elongate body, the presence of two dorsal fins with fin spines, and the elongate head had already been described. Based on spectacularly well-preserved fossils, we add new anatomical information on its exact body proportions, the paired and caudal fins, the dermal denticles, the skull morphology, the endocast, and the gill skeleton. These new skeletons from the Famennian (Upper Devonian) of Morocco (c. 367 Ma) permit a much-improved reconstruction of the anatomy of *Phoebodus*. The new materials comprise the oldest elasmobranch specimens preserving the complete head in three dimensions. Additionally, the new materials yield information about growth and diet and thus position in the trophic network. Despite the newly coded characters, the phylogenetic position of the genus *Phoebodus* with the oldest teeth dating to the early Givetian remains that of the oldest stem-elasmobranch in the Bayesian analyses.

Key words: Chondrichthyes, Elasmobranchii, Famennian, ontogeny, exceptional preservation, Fossillagerstätten.

Christian Klug [chklug@pim.uzh.ch; ORCID: https://orcid.org/0000-0002-4099-7453], Merle Greif [merle.greif@uzh.ch; ORCID: https://orcid.org/0000-0001-5519-017X], Jonathan Pople [jonathan.pople@pim.uzh.ch; ORCID: https://orcid.org/0009-0001-0029-0656], and Linda Frey [linda.frey@web.de; ORCID: https://orcid.org/0000-0001-6110-0548], Paläontologisches Institut, Universität Zürich, Karl-Schmid-Strasse 4, 8006 Zürich, Switzerland.
Alexander Pohle [alexander.pohle@rub.de; ORCID: https://orcid.org/0000-0001-6979-1048], Geowissenschaften, Ruhr-Universität Bochum, 44801 Bochum, Germany.
Michal Ginter [m.ginter@uw.edu.pl; ORCID: https://orcid.org/0000-0002-7210-7312], Faculty of Geology, University of Warsaw, Żwirki i Wigury 93, 02-089 Warsaw, Poland.
Michael I. Coates [mcoates@uchicago.edu; ORCID: https://orcid.org/0000-0003-2843-1075], Department of Organismal Biology and Anatomy, University of Chicago, 1027 E. 57th Street, Chicago, IL 60637, USA.
Wahiba Bel Haouz [wahiba.belhaouz@gmail.com; ORCID: https://orcid.org/0000-0002-4799-9697], Géosciences, Géomatique, Planétologie and Environnement (GEOPEN) laboratory, Department of Geology, Faculty of Sciences Ain Chock, Hassan II University, Km 8 Route d'El Jadida, 20100, Casablanca, Morocco.
Abdelouahed Lagnaoui [Abdelouaed.lagnaoui@uhp.ac.ma; ORCID: https://orcid.org/0000-0002-4176-1987], Laboratory of Education, Sciences and Training – LEST, Higher School of Education and Training Berrechid (ESEFB), Hassan First University, Route de Casablanca Km 3.5, BP 539, 26100, Berrechid, Grand-Casablanca, Morocco. Laboratory of Stratigraphy of Oil-and-Gas Bearing Reservoirs, Department of Paleontology and Stratigraphy, Institute of Geology and Petroleum Technologies, Kazan (Volga Region) Federal University, Kremlyovskaya Str. 18, Kazan, 420008, Russia.

Received 16 September 2026, accepted 24 April 2026, published online 30 June 2026.

Introduction

With the increasing number of three-dimensionally preserved Devonian vertebrate skulls and their endocasts revealed by computed tomography, our picture of evolutionary processes and anatomy of placoderms, chondrichthyans and osteichthyans is rapidly improving. After the evolution of jaws (Janvier 1996; Klug et al. 2017; Miyashita et al. 2025) over 435 Ma ago in the Silurian (Brazeau 2009; Brazeau and Friedman 2015; Zhu et al. 2013, 2022) or possibly even in the Ordovician (Zhu et al. 2022), new clades evolved rather quickly within the Silurian comprising the origins

of all major groups of jawed fish including Placodermi, Osteichthyes (actinopterygians plus sarcopterygians), and Chondrichthyes (Zhu et al. 2009; Brazeau and Friedman 2015; Andreev et al. 2022).

The first increase in diversity, disparity and abundance of gnathostomes occurred in the Silurian (Li et al. 2021; Zhu et al. 2021; Andreev et al. 2022) and intensified in the Devonian (Klug et al. 2010, 2023). Among cartilaginous fish, important cladogenic events happened during this interval (Coates et al. 2018; Frey et al. 2019b, 2020; Klug et al. 2023), bringing forth the chondrichthyan crown clade, defined by the divergence of the elasmobranch (sharks, skates, rays) and holocephalan lineages (chimaeras). Some of the oldest representatives of which have been documented from Morocco in the past decade based on exceptionally preserved fossils.

In the Moroccan Anti-Atlas, most major groups of Late Devonian jawed fish are well-represented, although the Gogo Formation in Western Australia (Long and Trinajstic 2018), the Escuminac Formation at the Canadian Miguasha (Schultze and Cloutier 1996), and the Cleveland Shale of Ohio (Carr and Jackson 2008) yielded a much greater diversity of Frasnian and Famennian gnathostomes. With the Kellwasser mass extinction in the late Frasnian, marine vertebrate assemblages experienced a profound turnover (Sallan and Coates 2010). Accordingly, it is not surprising that the Famennian Cleveland Shale fauna shares many more genera with the Moroccan Famennian faunas than to the Australian fauna of Frasnian age. However, the effects of the Kellwasser extinction were less severe than those of the end-Devonian Hangenberg Event. The palaeogeographical proximity (Kocsis and Scotese 2020) of the Famennian marine basins of the Anti-Atlas and Ohio certainly also contributed to that similarity. Concerning the skeletal fossil record of Famennian chondrichthyans from the eastern Anti-Atlas, *Maghriboselache* (Klug et al. 2023) is by far the most common genus, followed by *Phoebodus* (Frey et al. 2019a, b). In younger strata of the late middle and the late Famennian, remains of the largest Devonian shark *Ctenacanthus* are moderately common (a few skeletons and some isolated teeth; Greif et al. 2022, 2025). Two partial skeletons of *Symmorium* (or a closely related taxon; work in progress by MG and CK) are available and *Ferromirum* is represented by only its holotype (Frey et al. 2020). The tooth fossil record of Famennian chondrichthyans is predictably better but still poor (Derycke 1992; Ginter et al. 2002; Schnetz et al. 2022, 2024). *Phoebodus* is a very widely distributed genus, and its teeth have been found in many countries in Europe, Asia, Australia and northern America (Ginter et al. 2002, 2010), often in great abundance. They are characterized by three main cusps of similar size, often with one minute cusp in between two large cusps.

Recently, the phoebodontids were recognized as the earliest representatives of the elasmobranchs since isolated teeth are known from the early Givetian (Kaufmann 1998; Frey et al. 2019a). This insight was based on an approximately 60% complete skeleton of the late Devonian *Phoebodus saidselachus* from the Moroccan Anti-Atlas. The holotype of this species preserves the head region including the branchial skeleton, the shoulder girdle, somewhat questionable remains of the pelvic fins, the outline of the body including a few integumental remains but excluding the caudal region, and remains of both dorsal fins including fin spines. This specimen measures about 1.10 m in length.

Here, we describe six middle Famennian skeletons of *Phoebodus saidselachus*, which not only fill most gaps in anatomical knowledge about the skeletal anatomy and the dentition the type material had left, but which also yield some information about growth, adult body size and prey of this early elasmobranch. With the more complete anatomical knowledge, we test the phylogeny published by Frey et al. (2019a).

Institutional abbreviations.—B ESEFB, Higher School of Education and Training Berrechid, Hassan First University, Grand-Casablanca, Morocco; PIMUZ, Department of Palaeontology of the University of Zurich, Switzerland.

Geological setting

All six specimens (B ESEFB-LTM-203, PIMUZ A/I 4712, 5751–5754), were discovered in the southern Maïder in the eastern Anti-Atlas between the towns of Fezzou and Tafraoute Sidi Ali (Fig. 1). They were extracted from the Thylacocephalan Layer, an iron rich claystone with abundant flat ironstone concretions (Frey et al. 2019b). Many of these concretions contain exceptionally preserved specimens of the thylacocephalan crustacean *Concavicaris submarinus* (Jobbins et al. 2020). Variably complete skeletons of chondrichthyans, arthrodires and rarely osteichthyans occur in the same strata in large flat nodules, where the skulls are usually encased in the thickest part of the concretion (Frey et al. 2019b). In many cases, the concretions wedge out caudally; therefore, the caudal fin is often weathered away and only known from very few specimens. The cartilage is sometimes preserved in iron minerals and more often phosphatized. The same applies to soft tissues such as muscle remains, spiral valve, liver, kidney, etc. Remarkably, the Maïder fishes tend to have their soft tissues preserved in iron minerals while those of the southern Tafilalt are often phosphatized (Frey et al. 2019b). The mode of preservation and completeness also depends on the surface exposure of the different parts of the concretion. For example, the skull of PIMUZ A/I 5751 is missing due to erosion. The cartilage, fin spines, dermal denticles, and teeth are preserved in calcium phosphates, while soft tissue-remains are preserved in iron-bearing minerals including mainly haematite and limonite (Frey et al. 2019b).

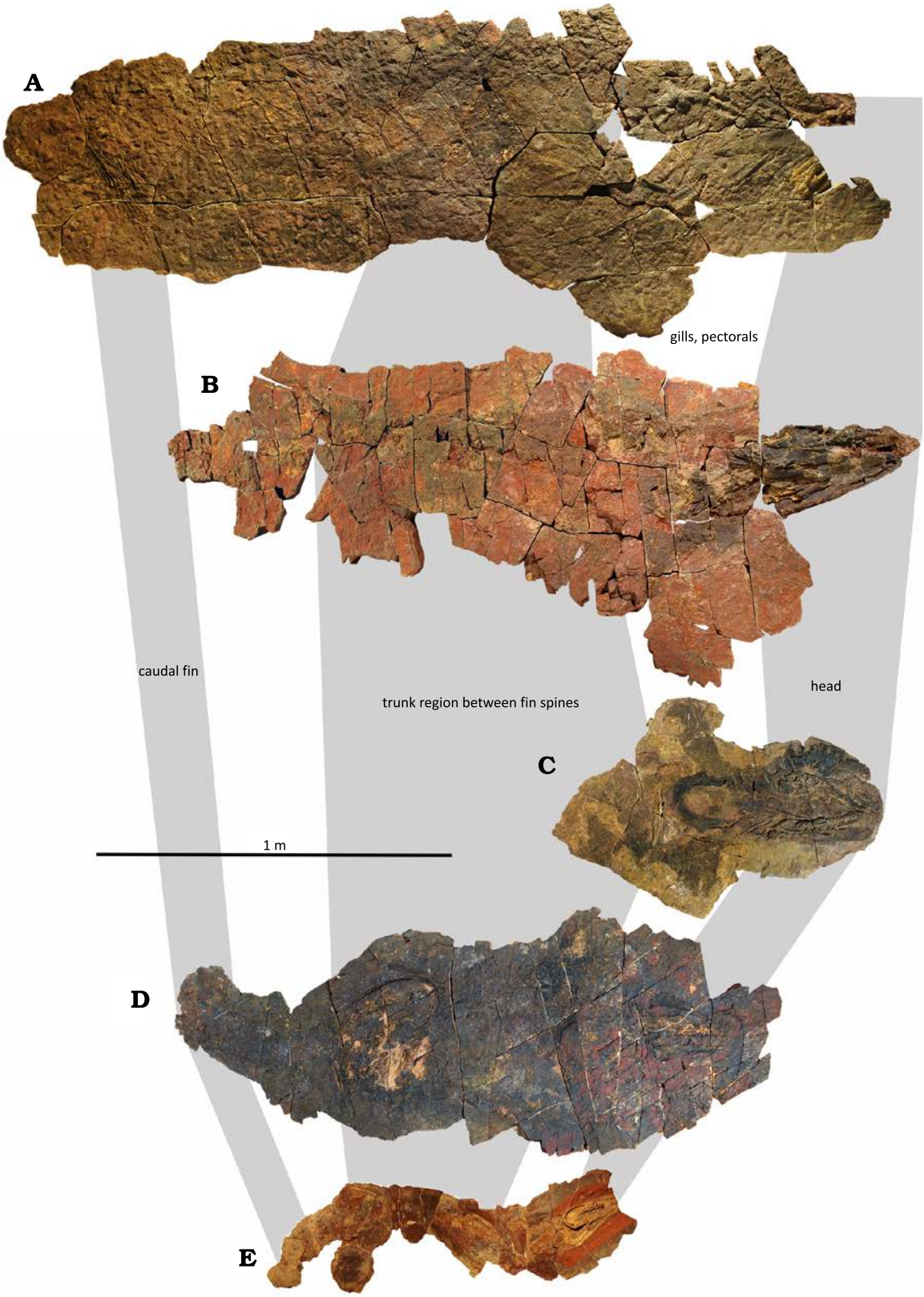

Fig. 1. Phoebodontiform elasmobranch *Phoebodus saidselachus* Frey et al., 2019a, middle Famennian, Upper Devonian, southern Maïder, Anti-Atlas, Morocco. **A**. PIMUZ A/I 5751, prep. T. Imhof, largest individual, nearly complete. **B**. PIMUZ A/I 5752, prep. T. Imhof, second largest individual, only caudal region missing; for details of the skull see Fig. 2. **C**. PIMUZ A/I 5753, prep. M. Greif, anterior half, excellent integument, fins and brachial region. **D**. PIMUZ A/I 5754, prep. R. Roth, two superimposed chondrichthyans; the skull in the middle is *Maghriboselache mohamezanei* with further remains; the straight, complete skeleton belongs to *Phoebodus*; the latter preserves the caudal fin. **E**. PIMUZ A/I 4712, holotype, smallest skeleton, nearly complete, modified after Frey et al. (2019a).

Material and methods

Material.—In this study, we include information from both the specimens included in Frey et al. (2019a) and newly prepared specimens. These include the isolated skull B ESEFB-LTM-203 and four more or less complete skeletons PIMUZ A/I 5751–5754 with different degrees of disarticulation. All specimens were extracted from the upper lower Famennian of the eastern Anti-Atlas. All specimens are kept at the Department of Palaeontology of the University of Zurich, Switzerland (PIMUZ), and at the Higher School of Education and Training Berrechid (ESEFB), Hassan First University, Berrechid, Grand-Casablanca (B ESEFB), Morocco.

Computed X-Ray Tomography.—B ESEFB-LTM-203 was scanned using computed tomography at Eurofins Qualitech AG (Mägenwil, Switzerland) with a 600 kV minifocus and the flat panel detector XRD 1621 AN18 ES. The reconstruction of the digital stack (1363 TIFF slices with a resolution of 995 × 1549 pixels) for virtual three-dimensional reconstruction was done by AP using MIMICS Innovation Suite 25.0 (Materialise NV, Leuven, Belgium). The density contrast between fossil cartilage and matrix varies strongly (mix of haematite, limonite and calcite), which made the segmentation very difficult, thus accounting for the poor quality of the renderings. The segmented models created in MIMICS were exported as PLY files. These were then imported into Blender 4.4.0 and smoothed using a Smooth modifier (Factor = 1.00, Repeat = 20), followed by a Displace modifier without a texture (Strength = 2.50) to counteract the shrinkage caused by the smoothing. The 3D models were rendered in Blender using the Cycles render engine. The image stack, the Mimics-file and ply-files of all segmented elements are available on Zenodo.

We did not scan the more complete head of PIMUZ A/I 5752 because it is deformed and extremely fragile; thus, it cannot be positioned with the rostral apex uppermost to allow effective X-ray penetration.

Phylogenetic methods.—We tested whether the new anatomical details have an influence on the phylogenetic position of *Phoebodus* as it was published by Frey et al. (2019a). We used the slightly modified matrices of Coates et al. (2017) with the modifications of Frey et al. (2019a, 2020) and Klug et al. (2023), which comprises 230 characters of 66 taxa. We also assessed phylogeny using the matrix of Bronson et al. (2024), where we added *Phoebodus* as well as *Maghriboselache*; this matrix contains 222 characters of 49 taxa. Notably, the choice of the taxa differs in all parts of the obtained trees, thus accounting for some of the differences in the results. We also changed a few scorings in the Bronson et al. (2024) matrix: 7 to 10 (*Kawichthys*: now ?), 20 (*Ozarcus*: now ?), 22 (*Ozarcus*: now 0), 47 (*Phoebodus*: now 1), 92 (*Phoebodus*: now 1), 108 (*Phoebodus*: now 1), 114 (*Phoebodus*: now 1), 115 (*Phoebodus*: now 2), and 191 (*Phoebodus*: now 1). Also note that the scoring as 2 or 3 of characters 50, 55, 56, 159, 160, 161, 162, 184, 218, 221 was provided like this by Bronson et al. (2024) in Morphobank. This might be an artifact from their work but should not alter the results.

The character matrix was analysed using RevBayes 1.2.5 (Höhna et al. 2016), using the fossilized birth-death model (Stadler et al. 2010; Gavryushkina et al. 2014; Heath et al. 2014). Extinction, speciation and fossil recovery rates were each drawn from an exponential prior with lambda = 10. For the root, we applied a uniform prior between 486.9 and 432.9 Ma (i.e., between the base of the Early Ordovician and the base of the Wenlock). This corresponds to the origin of the gnathostome crown group according to divergence time estimates from molecular data (e.g., Irisarri et al. 2017; Simakov et al. 2020) and accounts for *Shenacanthus*, the oldest known fossil chondrichthyan (Zhu et al. 2022). For the morphological characters, we used the MkVP+G model (see Mulvey et al. 2025), which is a modification of the Mk model (Lewis 2001), accounting for ascertainment bias, (i.e., invariant site correction; Lewis 2001), partitioned by the number of character states (Khakurel et al. 2024) and allowing for among-character variability in substitution rates (Yang 1994). For the latter, we used a discretised gamma distribution with four rate categories, using an exponential prior with lambda = 1.0 on the shape parameter alpha. We used a relaxed lognormal clock to model variable rates across branches, with an exponential prior (lambda = 1.0) on the mean and a gamma prior on the standard deviation ($\alpha = 0.5396$, $\beta = 0.3819$). We further allowed for variable dates (Barido-Sottani et al. 2019). The MCMC chains were run for four independent replicates of 25 000 generations using a random move schedule sampling every 10 generations, with 25% of the samples discarded as burn-in. Convergence was checked in Tracer (Rambaut et al. 2018), with all parameters reaching ESS above 200. We also performed parsimony analyses using both matrices and provide the results using the two matrices, analysed in TNT v. 1.6 (Goloboff and Morales 2023). All output files of Bayesian and parsiomony-analyses are freely available on Zenodo.

We changed the scoring of the following characters in the matrix produced by Coates et al. (2017) and modified by Frey et al. (2019a, 2020) and Klug et al. (2023):

22. Sclerotic ring: 0, absent, because none of the otherwise exceptionally preserved neurocrania show remains, even the perfectly 3D-preserved ones.

23. Sclerotic plate number: -, does not apply because there is no sclerotic ring.

56. Hypohyals: 1, present.

64. Long posterior copula: 1, long.

73. Number of generative tooth sets per jaw ramus: 0, 15 tooth sets.

97. Dental trough adjacent to oral rim on Meckel's cartilage and palatoquadrate: 1, present.

107. Palatobasal (or orbital) articulation posterior to the optic foramen: 1, absent.

108. Supraorbital shelf broad with convex lateral margin: 0, absent.

113. Ophthalmic foramen in anterodorsal extremity of orbit communicates with enclosed
cranial space: 0, absent.
126. Jugular canal diameter: 1, large.
130. Trigemino-facial recess: 1, present.
145. Endocranial roof anterior to otic capsules domelike, smoothly convex dorsally and anteriorly: 0, absent.
147. Roof of the endocranial space for telencephalon and olfactory tracts offset ventrally relative to level of mesencephalon: 0, absent.
151. Angle of external semicircular canal: in lateral view, straight line projected through canal intersects anterior ampulla, external ampullae, and base of foramen magnum: 0, absent.
160. External opening for endolymphatic ducts anterior to crus commune: 0, absent.
164. Endolymphatic fossa: 0, absent.
165. Endolymphatic fossa elongate (slot-shaped), dividing dorsal otic ridge along midline: 0, absent.
182. Chordacentra: 0, absent.
193. Scapular process with posterodorsal process. 1, present.
196. Procoracoid mineralisation: 1, present
213. Caudal radials extend beyond level of body wall and deep into hypochordal lobe: 1, present.

Systematic palaeontology

Chondrichthyes Huxley, 1880

Elasmobranchii Bonaparte, 1838

Phoebodontiformes Ginter et al., 2010

Genus *Phoebodus* St. John & Worthen, 1875

Type species: *Phoebodus sophiae* Ginter et al., 2010, Givetian–Famennian; distribution nearly cosmopolitan.

Emended diagnosis (modified after Frey et al. 2019a).—Tooth sets separated by gaps; individual teeth with crown bearing three long main cusps with sigmoid profile, equally sized or with median cusp slightly shorter; short intermediate cusplets occasionally present; base symmetric; single orolingual button on lingual torus; arcuate basolabial projection; single aboral and lingual basal canal openings. Jaws amphystylic; otic process of the palatoquadrate dorsoventrally short, longer than the palatal part; ceratohyal anteriorly blade-shaped; pharyngeal teeth present. Otic division of braincase twice as long as the elongate occipital region; hypotic lamina massive. Pointed rostrum extending anteriorly in front of the jaws. Juvenile body slender, adult moderately slender. Integument bearing multicuspid body denticles with rhomboid shape; two dorsal fins, each with calcified base plates and fin spines with crenulated costae.

Stratigraphic and geographic range.—Middle and Late Devonian of Africa, Australia, Eurasia, and northern America.

Phoebodus saidselachus Frey et al., 2019a

Figs. 1–21.

Holotype: PIMUZ A/I 4712, nearly complete skeleton.
Type locality: Madene El Mrakib, Morocco.
Type horizon: Middle Famennian, Upper Devonian.

Emended diagnosis (modified after Frey et al. 2019a).—Mandibular teeth with main cusps recurved lingually, of nearly identical length, each with two distinct striae forming sharp edges; lateral cusps with broader diameter than the median; two intermediate cusplets reach almost half central cusp length and thickness; tooth base squarish with rounded angles in aboral view; base outline concave in labial and aboral aspects; the basolabial projection wider than the median cusp and labiolingually narrow. Neurocranium elongate with a flat and triangular rostrum; endocast chambers for telencephalon, mesencephalon and cerebellum of similar thickness; semicircular canals moderately thick but anterior and posterior semicircular canals forming a low arch; all three canals are narrowly wrapped around the cerebellum. Dorsal fin spines with gentle posterior curvature; basal opening extends to at least 50% of total height; insertion deep; ornament of fine ctenoid ridges. Anterior fin spine much more triangular, inserted at a lower angle than the slenderer posterior fin spine.

Material.—PIMUZ A/I 5751, caudal fin, both dorsal fin spines as external moulds and the branchial arches. Most of the skull except the posterior part of the jaws with two teeth had weathered away, from Khrabis (30.759160 N, 4.709635 W), Morocco, Thylacocephalan Layer, middle Famennian.

PIMUZ A/I 5752, a slightly deformed head , with a brachiopod preserved on the lower jaw in life position confirming that the shark carcass had settled on its dorsum, from Rich Bel Ras, south of Jebel Oufatene (30.810675 N, 4.875930 W) , Morocco, Thylacocephalan Layer, middle Famennian.

PIMUZ A/I 5753, the front half of the skeleton in ventral view with well-preserved branchial basket, pectoral girdle and much of the dermal denticles of the pectoral region, lingual side of the left Meckel's cartilage, a small chondrichthyan fin spine, 7 costae and the trailing edge shows curved denticles, excellently preserved integument in the pectoral region is contrasted by the missing posterior portion of the body, from Madene El Mrakib, between Tafraoute Sidi Ali and Nkoub Krabis (30.729708 N, 4.721857 W) , Morocco, Thylacocephalan Layer, middle Famennian.

PIMUZ A/I 5754, remains of two flattened skeletons on a slab: head (and possibly scapulocoracoid and pectoral fin) of *Phoebodus saidselachus* and skull of *Maghriboselache mohamezanei*, from Madene El Mrakib, between Tafraoute Sidi Ali and Nkoub Krabis (30.738126 N, 4.720373 W), Morocco, Thylacocephalan Layer, middle Famennian.

B ESEFB-LTM-203, skull (jaw elements and the neurocranium are articulated, tip of the snout and anterior parts of the Meckel's cartilages are missing), from Madene El Mrakib

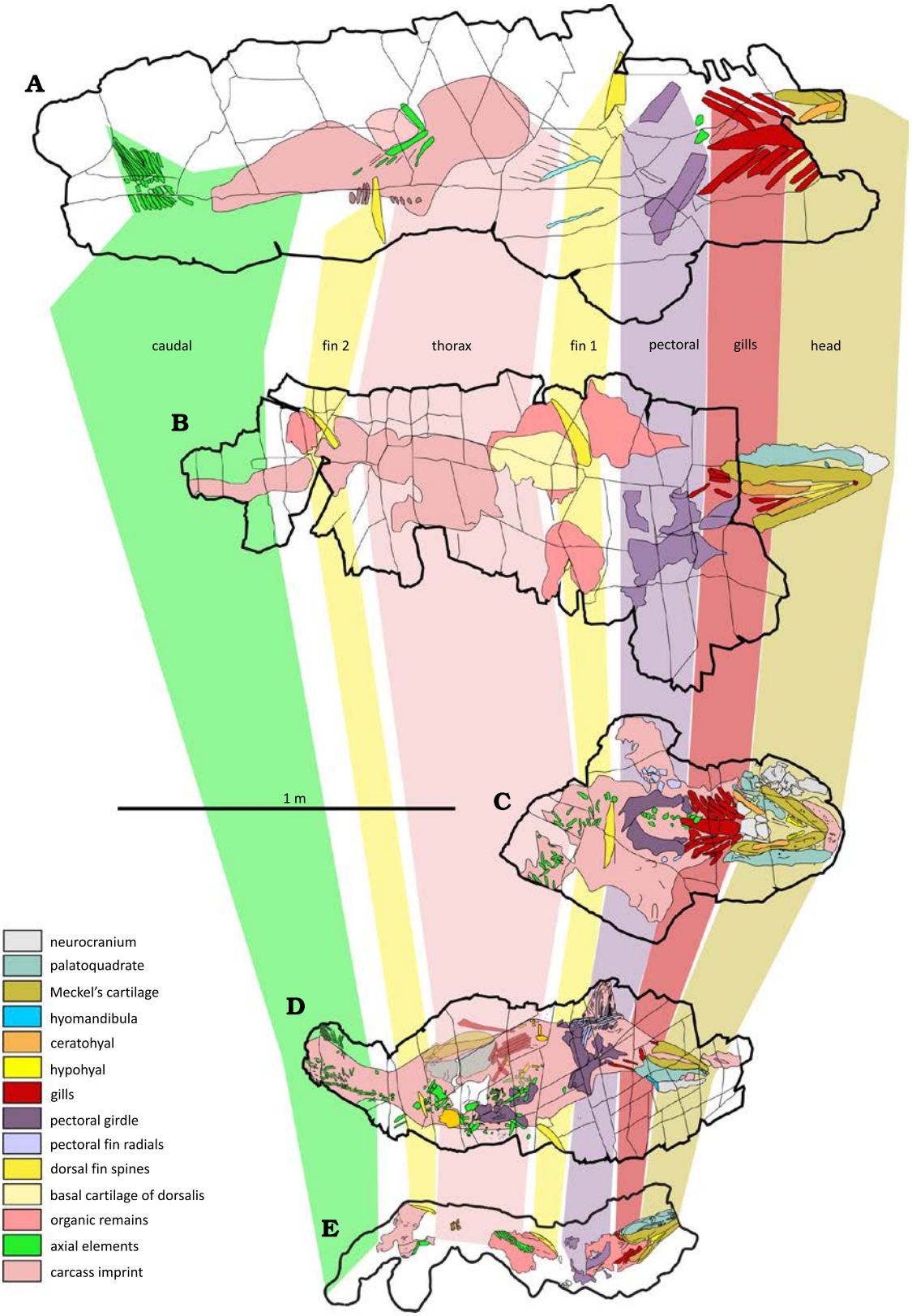

Fig. 2. Interpretative sketches of the phoebodontiform elasmobranch *Phoebodus saidselachus* Frey et al., 2019a, middle Famennian, Upper Devonian, southern Maïder, Anti-Atlas, Morocco. All specimens lie on their back. **A**. PIMUZ A/I 5751, largest individual, most of the skull is missing, otherwise complete. **B**. PIMUZ A/I 5752, second largest individual, nearly 3D-skull, caudal region missing. **C**. PIMUZ A/I 5753, only anterior half, integument with articulated denticles, perfect fins and brachial region. **D**. PIMUZ A/I 5754, prep. R. Roth, two superimposed chondrichthyans; the skull in the middle is a cladoselachid with further remains; the straight, complete skeleton belongs to *Phoebodus saidselachus*; the latter preserves the caudal fin. **E**. PIMUZ A/I 4712, holotype, nearly complete skeleton, currently the shortest, modified after Frey et al. (2019).

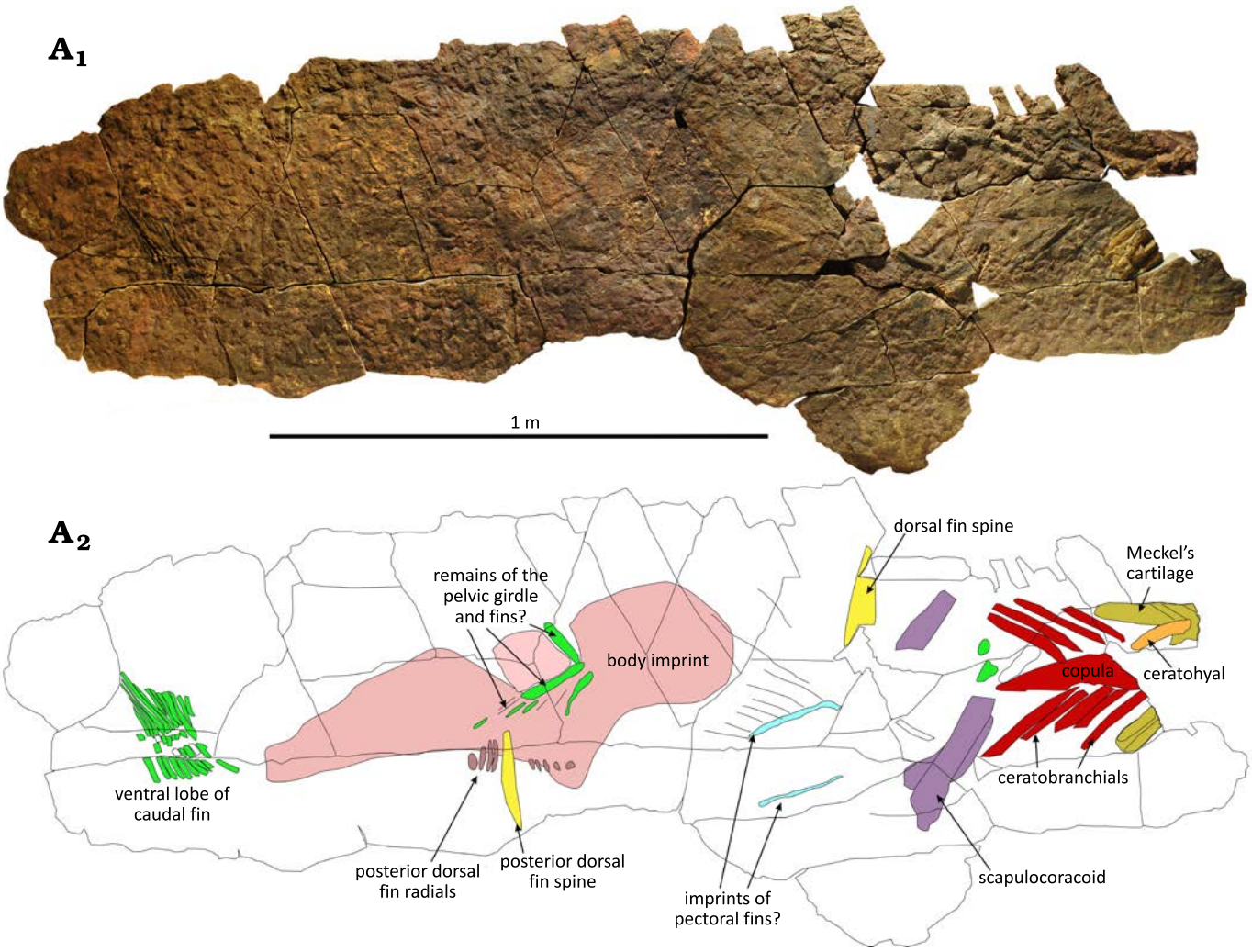

Fig. 3. Photo (A_1) and interpretative line drawing (A_2) of the phoebodontiform elasmobranch *Phoebodus saidselachus* Frey et al., 2019 (PIMUZ A/I 5751), middle Famennian, Upper Devonian, southern Maïder, Anti-Atlas, Morocco. Posterior end of cranium, dorsal fins with fin spines and caudal fin are reasonably well preserved. The ventral part of the branchial basket is nearly complete while the shoulder girdle and paired fins are absent or very fragmentary.

(30.440407 N, 4.420899 W) , Morocco, Thylacocephalan Layer, middle Famennian.

Description.—All skeletons are from carcasses that had settled mostly obliquely on their backs on the sediment surface (Figs. 1, 2). Although the dorsal side is embedded in the nodule, torsion of the carcass often flipped some body parts on one side. The largest individual PIMUZ A/I 5751 measures 2.52 m in length (Fig. 3). The orientation of the two fin spines indicates that the carcass was twisted longitudinally. It preserves the caudal fin, both dorsal fin spines as external moulds and the branchial arches. Most of the skull except the posterior part of the jaws with two teeth had weathered away.

PIMUZ A/I 5752 is a skeleton that is 2.14 m long (Fig. 4). It preserves a slightly deformed, 0.45 m long head and misses the caudal fin. The head is excellently preserved.

Only the front half of the skeleton of PIMUZ A/I 5753 is present in ventral view with well-preserved branchial basket, pectoral girdle and much of the dermal denticles of the pectoral region (Fig. 5). The specimen is about 1.05 m long and the splayed pectoral fins span 0.64 m. On the lingual side of the left Meckel's cartilage, a small chondrichthyan fin spine is preserved (18 × 3.2 mm in size). It carries 7 costae and the trailing edge shows curved denticles that are about 0.7 mm long. Its size suggests that it derives from a prey chondrichthyan, perhaps the smaller ctenacanth *Acondylacanthus* (Lebedev et al. 2020: fig. 6). The excellently preserved integument in the pectoral region is contrasted by the missing posterior portion of the body. The change from articulated to chaotically arranged neural arches may suggest that the rear half was eaten (or scavenged) by a bigger predator (Greif et al. 2025). Alternatively, the carcass may have been incompletely buried initially, and putatively exposed body parts may have disarticulated over time because of weak bottom currents.

PIMUZ A/I 5754 preserves remains of two flattened skeletons on a slab of about 1.74 m length (Fig. 6). The two skeletons were identified by their dentition. The 180 mm

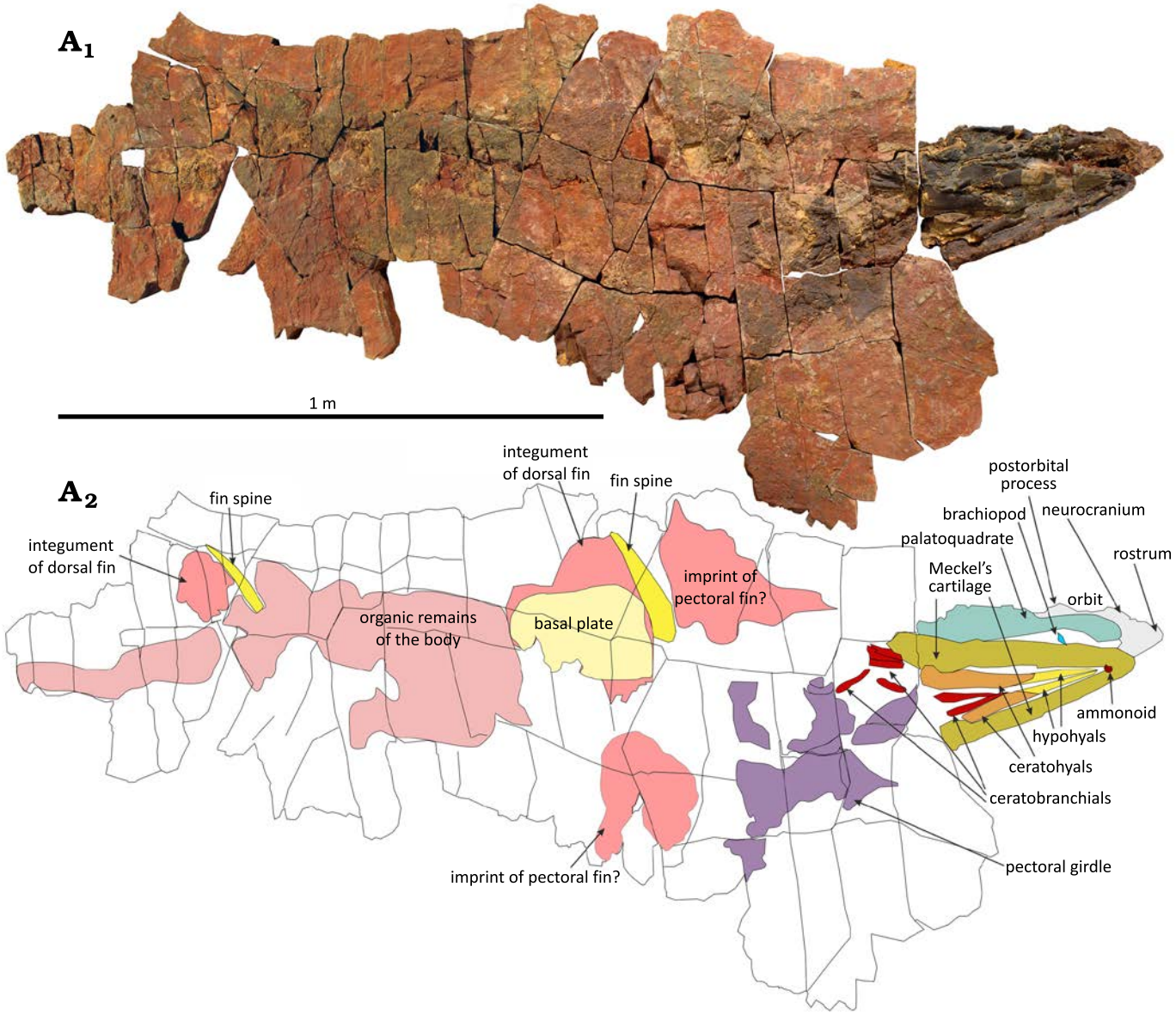

Fig. 4. Photo (A_1) and interpretative drawing (A_2) of the phoebodontiform elasmobranch *Phoebodus saidselachus* Frey et al., 2019a (PIMUZ A/I 5752), middle Famennian, Upper Devonian, southern Maïder, Anti-Atlas, Morocco. Skull and dorsal fins are well preserved. Caudal and ventral fins are not preserved.

long head of *Phoebodus saidselachus* points to the left in Figure 6. The second skull is in a central position and belongs to *Maghriboselache mohamezanei* (Klug et al. 2023). The *Phoebodus* skeleton is undulating around the *Maghriboselache*-skull and stretches over about 1.6 m. The attribution of the pectoral skeleton is uncertain because of the cluttered superposition of numerous cartilages. The scapulocoracoid and pectoral fin are positioned as if part of the *Phoebodus* skeleton, but the morphology of the girdle and fin radials resembles those of *Maghriboselache*. Also, the pectoral fin integument preserves monodontode denticles like those of *Maghriboselache* (Klug et al. (2023: fig. 9). Two smooth fin spines are exposed, but the absence of ornamentation suggests that they belong to *Maghriboselache*.

B ESEFB-LTM-203 preserves the skull only (Figs. 7–10). The skull is in an undeformed state and the jaw elements and the neurocranium are articulated. It is quite eroded: the tip of the snout and anterior parts of the Meckel's cartilages are missing. The skull is overgrown by an iron rich, laminated stromatolite-like structure. It might have been prefossilized and reworked, where the postcranial material was lost. It was then exposed and the iron crusts of perhaps microbial origin formed.

Head: The skull B ESEFB-LTM-203 preserves all cartilages and many of the teeth in situ (Greif et al. 2026). It is about 250 mm long (Fig. 7). Since the jaws are better preserved in PIMUZ A/I 5752 and A/I 5753, we focus here on the neurocranium and the endocast of B ESEFB-LTM-203.

The slender neurocranium of PIMUZ A/I 5752 (Fig. 4) is about 300 mm long and slightly distorted by compaction. At the postorbital processes, it is about 110 mm wide. The orbits are wedge-shaped, 125 mm long and up to 46 mm high

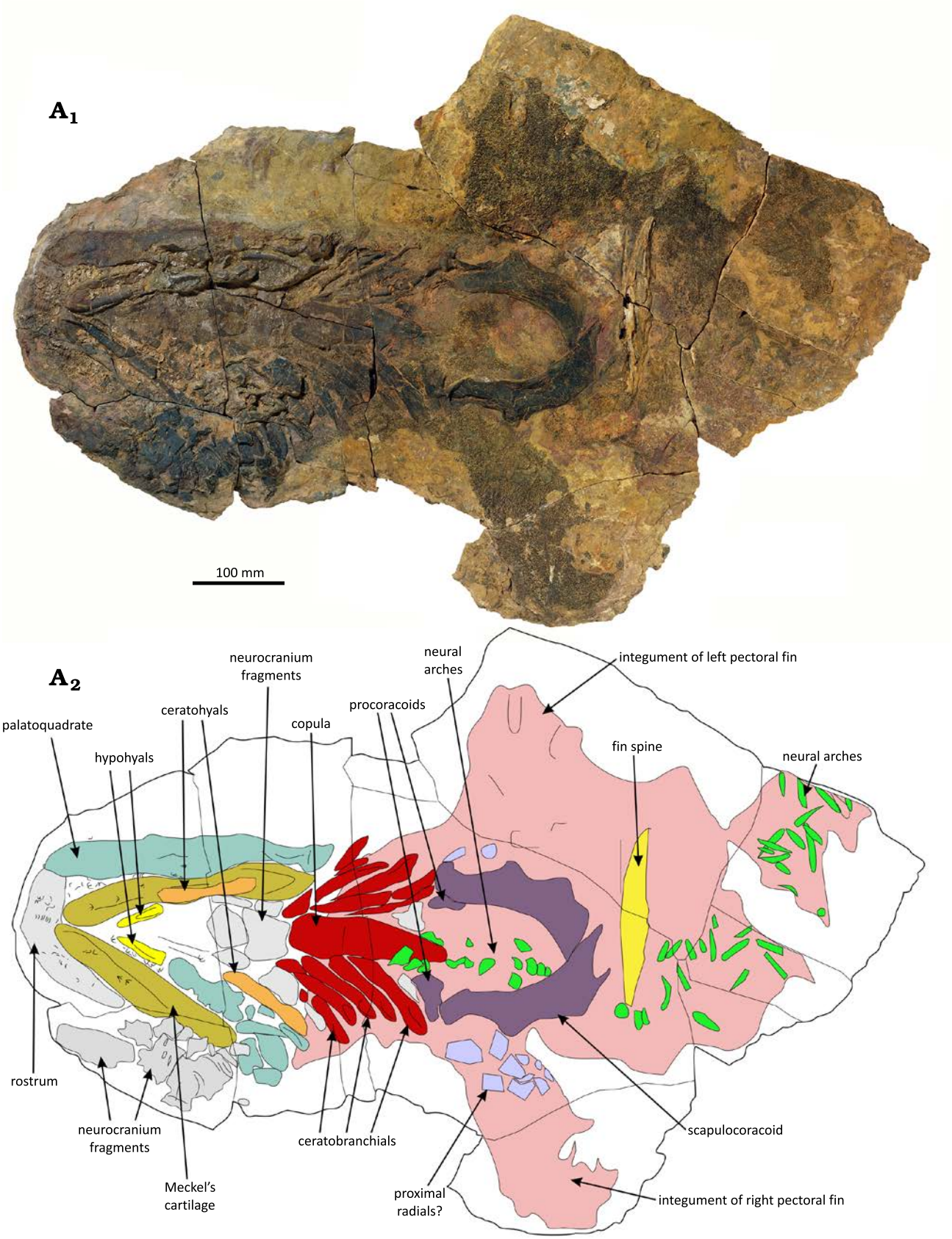

Fig. 5. Photo (A_1) and interpretative line drawing (A_2) of the phoebodontiform elasmobranch *Phoebodus saidselachus* Frey et al., 2019a (PIMUZ A/I 5753), middle Famennian, Upper Devonian, southern Maïder, Anti-Atlas, Morocco. Skull, pectoral girdle and fins as well as the anterior dorsal fin spine are well preserved. Note that the neural arches are dislocated towards the right.

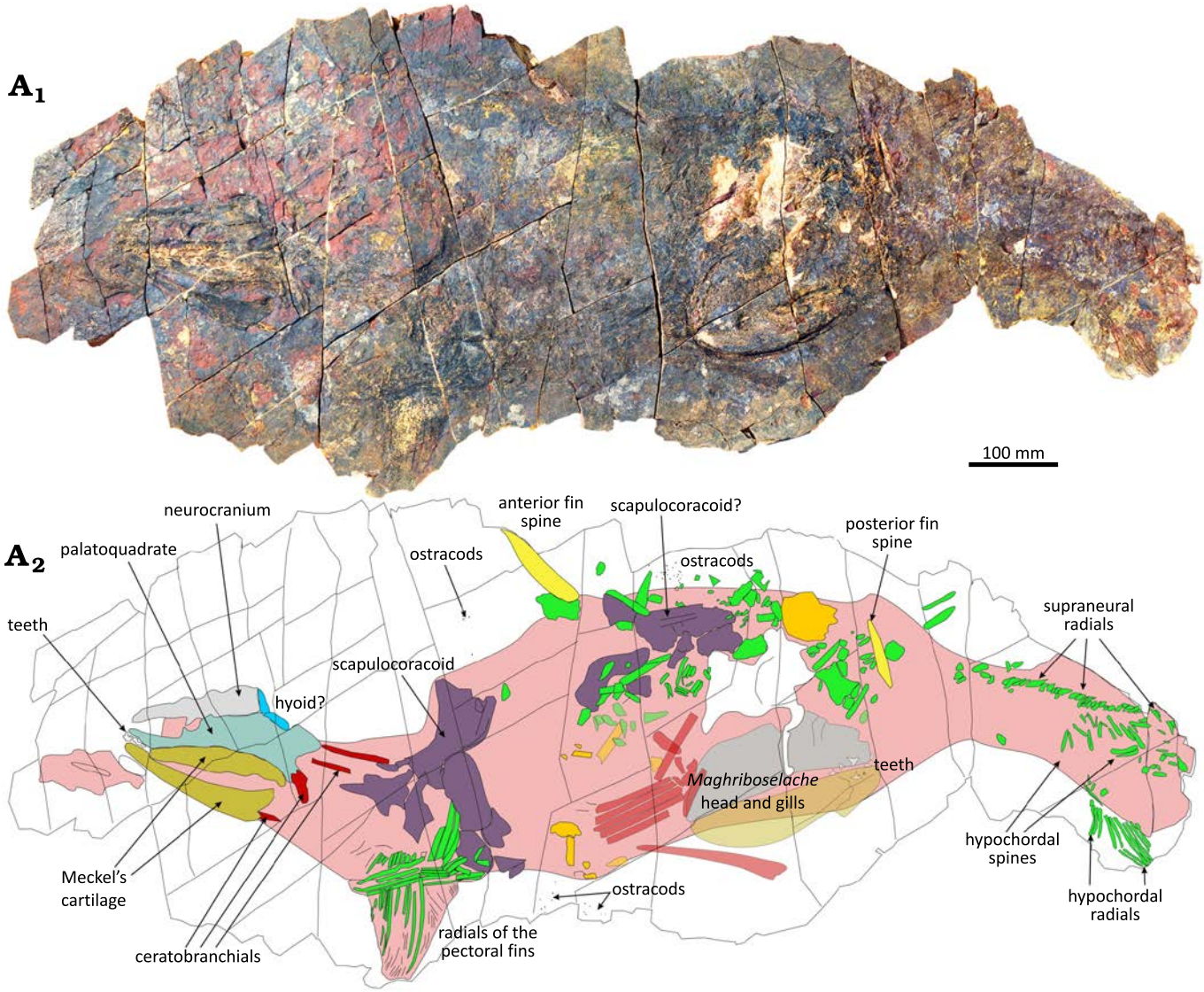

Fig. 6. Photo (A_1) and interpretative line drawing (A_2) of the phoebodontiform elasmobranch *Phoebodus saidselachus* Frey et al., 2019a (PIMUZ A/I 5754), middle Famennian, Upper Devonian, southern Maïder, Anti-Atlas, Morocco. This slab contains remains of two chondrichthyans: the slender head of *Phoebodus* is on the left, while the broader head of *Maghriboselache* lies more in the centre.

close to the postorbital process. In contrast to B ESEFB-LTM-203, PIMUZ A/I 5752 preserves the complete anterior tip of the rostrum with the nares. The rostrum is flat and pointed, giving its face an appearance reminiscent of the blue shark *Prionace glauca*. Anterior to the orbits, the flat and pointed parabolic rostrum is about 60 mm long. Except for rostrum and nasal chambers, the neurocranium of B ESEFB-LTM-203 is complete and hardly deformed. However, the sediment density changes drastically within the fossil and thus, in some places, the contrast was good, and segmenting was feasible, while in other parts, it was very difficult to differentiate between sediment and cartilage.

The orbits are oval, elongated in rostro-caudal direction, about 90 mm long and 45 mm high. The suborbital shelf is of similar width than the supraorbital shelf, which is perfectly flat. The openings of the optic nerves have a subcentral position in the orbits and in the posterior half of the orbits, the recesses that housed the pituitary veins are preserved (Figs. $7A_2$, A_4, $8A_2$, A_5). The optic pedicle is visible in B ESEFB-LTM-203 (Fig. $8A_2$, A_5). The orbital articulation is anterior to the optic foramen. Both postorbital processes could be segmented, although their lateral extremities had been weathered away. They are rather thin and dorsoventrally gently sigmoidally vaulted. They display the wide jugular canal (Fig. $8A_3$, A_6) dorsolaterally of the trigemino-facial recess. CT-images of the otic and the postotic regions have a very poor contrast, which rendered the segmentation very difficult. This part of the neurocranium has a ventral bulge of the lateral otic ridge and a smooth dorsal bulge until the occipital fissure, which is well visible on the right (Fig. $8A_5$). Due to erosion of the dorsal surface, the endolymphatic duct opens in a flat area, but likely, there used to be a bulge (Fig. $8A_5$).

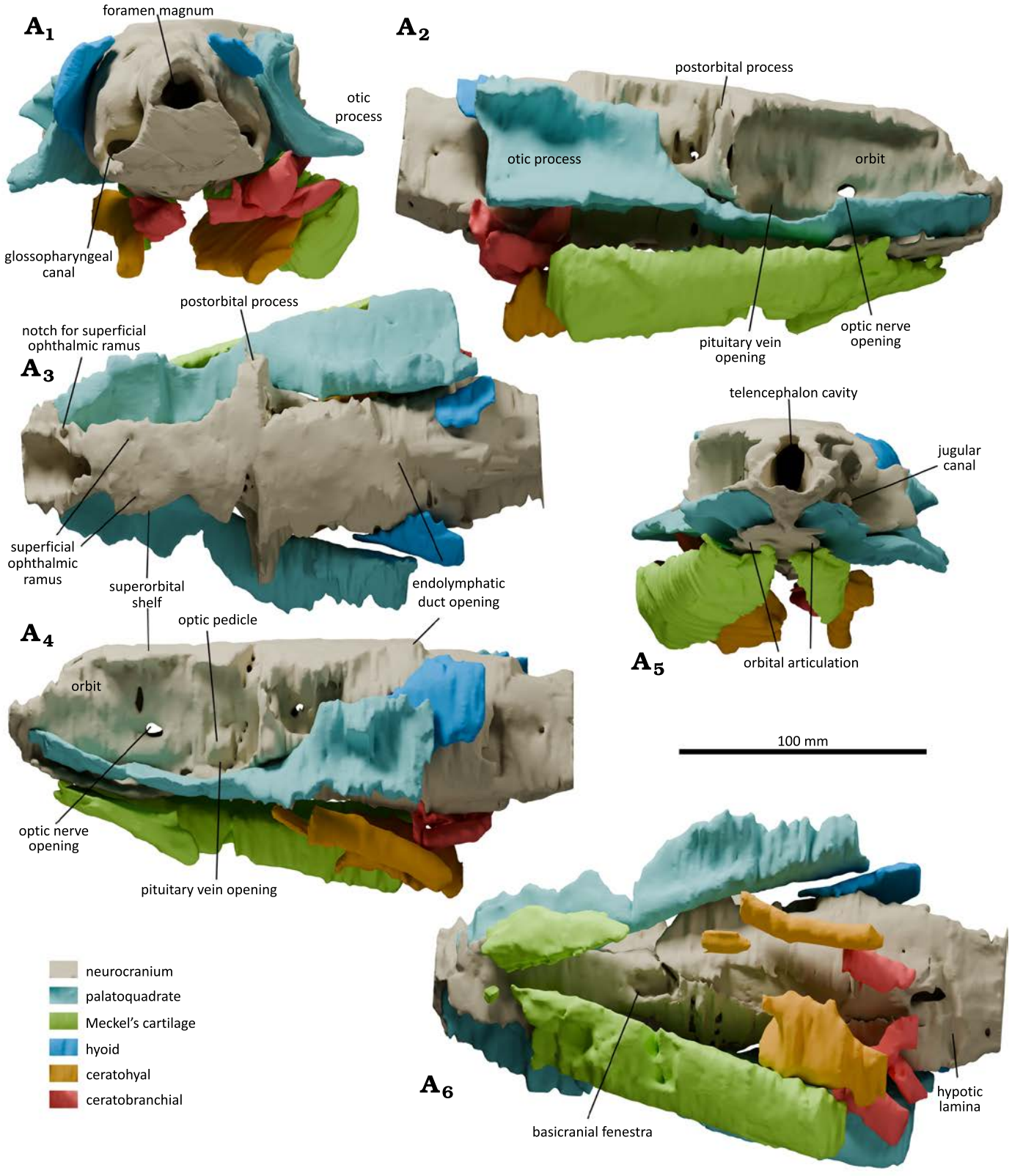

Fig. 7. The head of the phoebodontiform elasmobranch *Phoebodus saidselachus* Frey et al., 2019a (B ESEFB-LTM-203), middle Famennian, Upper Devonian, southern Maïder, Anti-Atlas, Morocco. Three-dimensional reconstructions of specimen in posterior (A_1), right side (A_2), dorsal (A_3), left side (A_4), anterior (A_5), and ventral (A_6) views. Note that the nasal capsules, the rostrum and parts of the Meckel's cartilages are eroded. All renderings are in orthographic view.

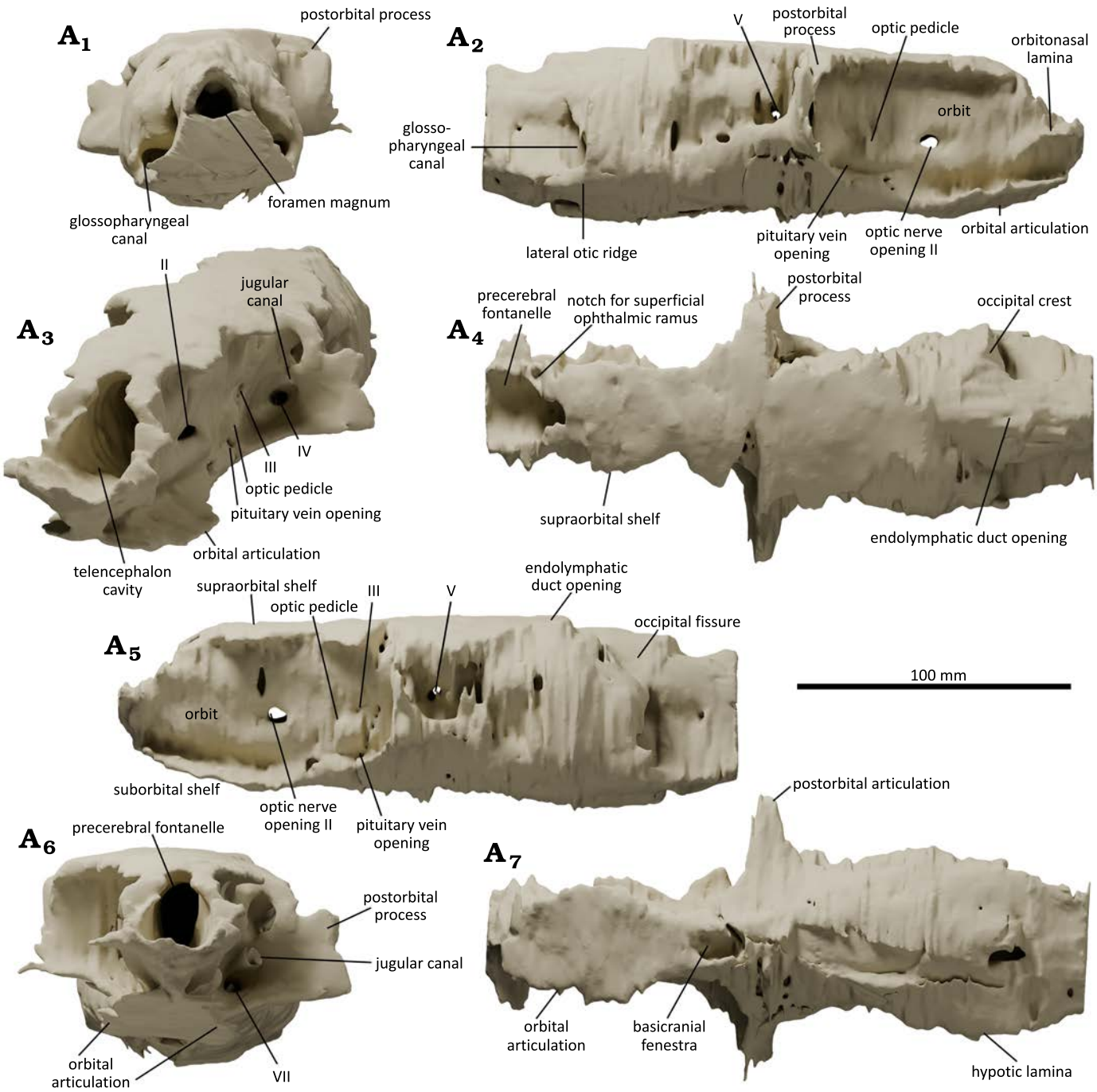

Fig. 8. The neurocranium of the phoebodontiform elasmobranch *Phoebodus saidselachus* Frey et al., 2019a (B ESEFB-LTM-203), middle Famennian, Upper Devonian, southern Maïder, Anti-Atlas, Morocco. Three-dimensional reconstructions of specimen in posterior (A_1), right side (A_2), oblique anterior (A_3), dorsal (A_4), left side (A_5), anterior (A_6), and ventral (A_7) views. Note that the postorbital processes, the nasal capsules and the rostrum are heavily eroded, and the contrast of the CT-images varies strongly between regions, hence the artifacts. All renderings, except A_3, are in orthographic view.

In contrast to the fragmentary endocast presented by Frey et al. (2019a: fig. 2), we can now describe almost the entire endocast, where only the nasal capsules are missing (Fig. 9). In B ESEFB-LTM-203, it is about 230 mm long and quite slender like the endocasts of *Orthacanthus* (Schaeffer 1981), *Cladodoides* (Maisey 2005), and *Maghriboselache* (Klug et al. 2023). Accordingly, the mesencephalon chamber is represented only by a subtle swelling (Fig. $9A_3$) and the cross section of the endocast changes only subtly; telencephalon, mesencephalon, cerebellum, and the brain stem spaces hardly change in cross sectional area and have the shape of a gently sinusoid tube. Perhaps the most striking feature is the very narrow arrangement of the semicircular canals, where the sagittal direction is quite pronounced, i.e., they are laterally

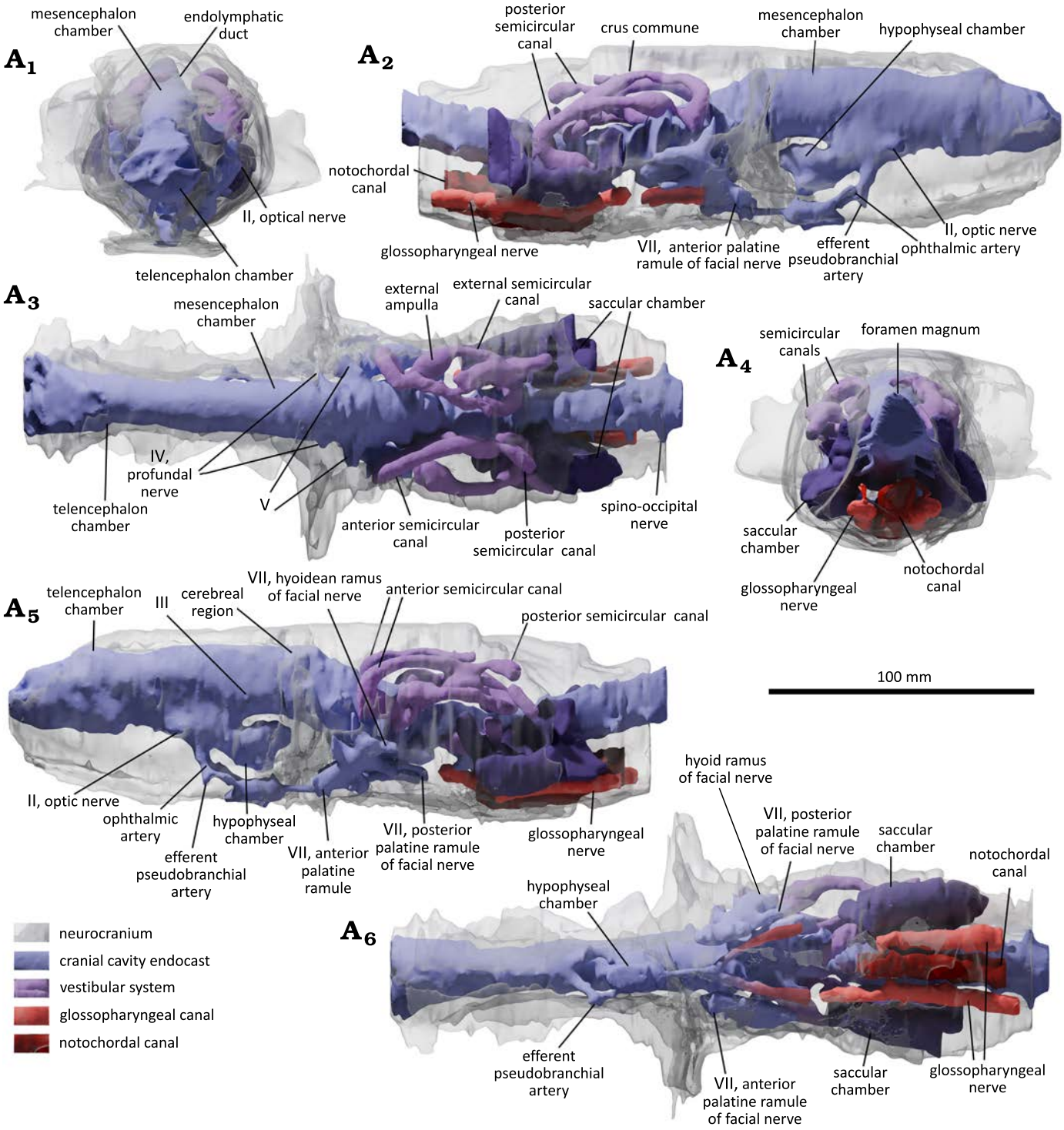

Fig. 9. The endocast of the phoebodontiform elasmobranch *Phoebodus saidselachus* Frey et al., 2019a (B ESEFB-LTM-203), middle Famennian, Upper Devonian, southern Maïder, Anti-Atlas, Morocco. Three-dimensional reconstructions of specimen in anterior (A_1), right side (A_2), dorsal (A_3), posterior (A_4), left side (A_5), and ventral (A_6) views. Note that the nasal capsules are eroded. All renderings are in orthographic view.

and dorsoventrally compressed compared to, e.g., species of *Dwykaselachus*, modern holocephalans, *Maghriboselache* and *Cladodoides* (Coates et al. 2017; Klug et al. 2023). In species of *Orthacanthus* and *Squalus*, the labyrinths are similar to *Phoebodus* with respect to the rather low height, the short sinus superior, short external semicircular canal, the lack of projections on the lateral extremity. There is some difference in the angle between the anterior and posterior semicircular canals, which is around 120° in *Orthacanthus*, about 95° in *Squalus* and about 140° in *Phoebodus*. The value of this angle is likely linked with the shape of the endocast in the cerebellar and otic regions, which widens in

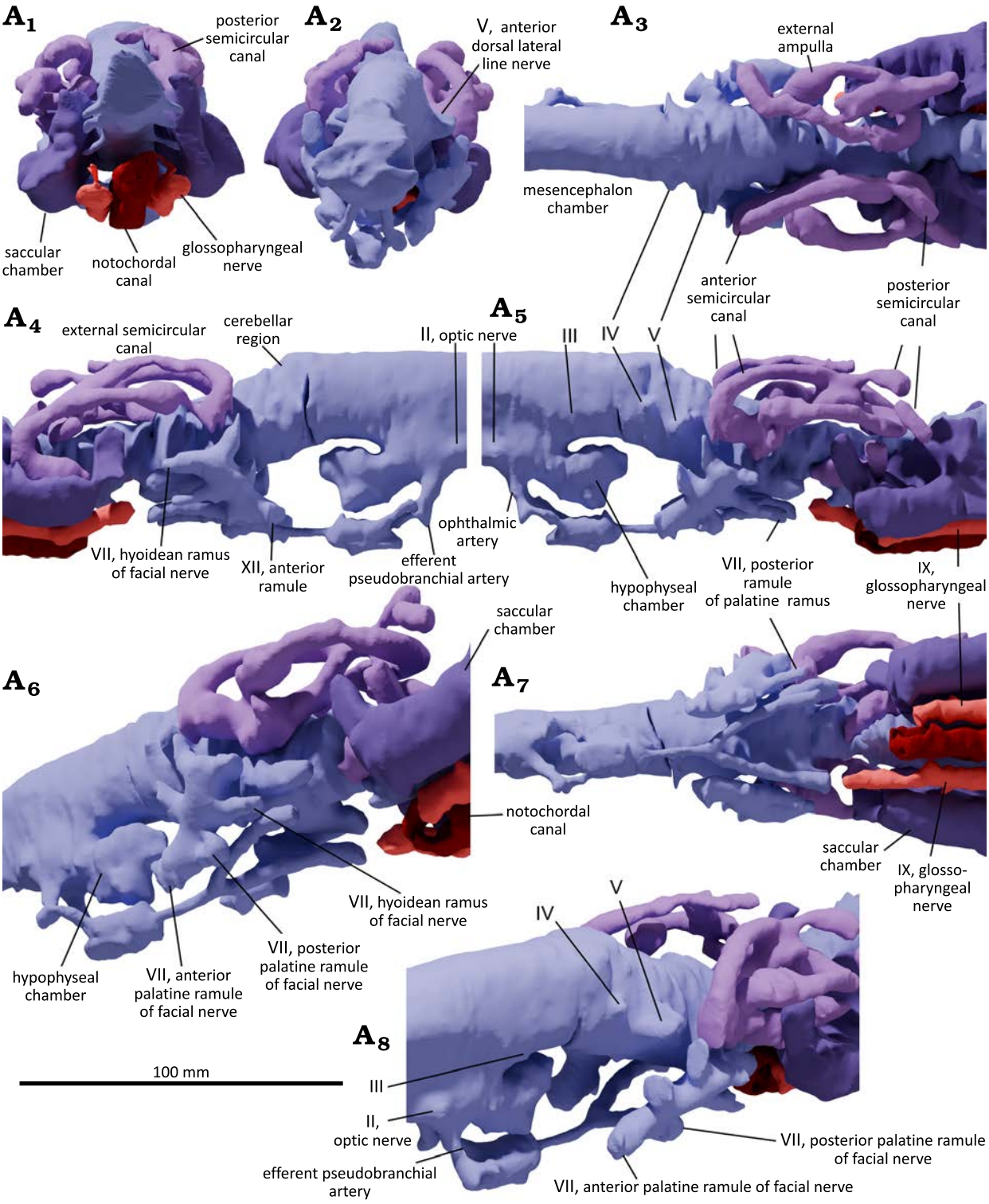

Fig. 10. Details of the endocast of the phoebodontiform elasmobranch *Phoebodus saidselachus* Frey et al., 2019a (B ESEFB-LTM-203), middle Famennian, Upper Devonian, southern Maïder, Anti-Atlas, Morocco. Three-dimensional reconstructions of specimen without the neurocranium transparent overlay in posterior (A_1), anterior (A_2), dorsal (A_3), right side (A_4), left side (A_5), left lateroventral (A_6), ventral (A_7), and antero-dorsolateral (A_8) views. Note that the nasal capsules are eroded. All renderings, except A_6 and A_8, are in orthographic view.

Orthacanthus and *Squalus*, while in *Phoebodus*, it hardly changes its width. The slender construction of the labyrinth is consistent with the overall narrow triangular shape of the head of *Phoebodus*. The ventral portion of the vestibular system (saccular and lagenar chamber, or pars inferior) is somewhat displaced posteriorly on both sides relative to the dorsal portion (canals, sinus superior, plus utriculus), probably by some taphonomic process (the specimen is overgrown

by microbial crusts, evidencing prolonged exposure at the sediment surface). The otic capsules have been damaged during taphonomy. The pars inferior is displaced backwards suggesting a breakage. The occipital part became somewhat separated and a crack runs through the otic capsules and canals as well as the basicranium. The hypophyseal chamber has a slightly reduced thickness compared to the telencephalon. The openings and endocasts of many cranial nerves such as the optic nerve, the octaval nerve, both the hyoid and the posterior palatine ramules of the facial nerve, the glossopharyngeal nerves, and the three ventral spino-occipital nerves could be visualized (Fig. 9). The dorsal inflection of the medullar chamber is another feature worth comparing to species of *Orthacanthus*. The dorsal inflexion of the medullar chamber of *Phoebodus* is much more important than that of species of *Orthacanthus*. It starts posterior to the otic capsules in species of *Phoebodus*, while in species of *Orthacanthus*, it lies at the level of the foramen magnum, probably because the latter opens more dorsally.

Mandibular arch: In PIMUZ A/I 5752, Meckel's cartilages, palatoquadrates and the neurocranium are perfectly articulated (Figs. 11, 12). The whole head is 450 mm long and thus one of the largest. Among the chondrichthyans known from Morocco, this species has the slenderest skull with a pointed rostrum. In contrast to B ESEFB-LTM-203, PIMUZ A/I 5752 preserves the complete anterior tip. The nose is flat and pointed, giving its face an appearance reminiscent of the blue shark *Prionace glauca*.

The left Meckel's cartilage of PIMUZ A/I 5752 is about 350 mm long and 80 mm high. The posterior ends are about 200 mm apart. These cartilages are rather straight with a very gentle inward curvature, which increases only from the last 30 mm behind the symphysis to the front. It holds 15 tooth families per ramus (Fig. 11A$_3$), where the seven preserved symphyseal teeth (central cusp 6 mm long) are smaller than the ones from the adjacent tooth families (central cusp 10 mm long; Fig. 11A$_2$). One small tooth from one of the posterior tooth rows measures only 4 mm in width, probably it was not fully developed yet. Between each tooth family, there is a gap approximately of the same width as the teeth or slightly less. Both ceratohyals are present, although their anterior edges are weathered. 175 mm of the right ceratohyal are preserved with both ends missing. It tapers towards the anterior from 32 mm to about 16 mm. All tooth families still rest in the tooth furrow and there is no evidence that teeth were retained (Williams 2001) after lateral (labial) displacement from a functional position in the gape. The small size-differences of teeth within a single family (or generative tooth set; see Botella 2006 and Botella et al. 2009) suggest that teeth were shed at a higher rate than in species of *Ctenacanthus* (Greif et al. 2025), *Symmorium* (MG and CK unpublished data) or *Maghriboselache* (Klug et al. 2023). This is further supported by only minimal traces of tooth wear, where the main cusps are only slightly rounded (Fig. 11A$_2$). Tooth replacement in *Phoebodus* and other Devonian chondrichthyans is under study by Greif et al. (2026).

The left palatoquadrate of PIMUZ A/I 5752 (Fig. 11A$_3$) is also about 350 mm long, although the anterior edge is only poorly visible. The otic process until the postorbital process is 220 mm long and up to 80 mm high. Its dorsal and posterior edge carries a thick, 20 mm high ridge. The anterior part of the ridge is slightly broadened and bears a shallow furrow directed posterolaterally. Once again, this is a feature shared with species of *Orthacanthus* (Hotton 1952) but is seemingly absent in ctenacanths (Ginter and Maisey 2007) and might have carried a branch of the hyomandibular branch of the facial nerve. Some tooth families are visible, but there is no visible difference to those of the lower jaw.

The skull of PIMUZ A/I 5753 is surrounded by some reasonably preserved polyodontode dermal denticles (Fig. 13). They vary in transverse width between 1 and 3 mm. They share an irregular rhomboid outline and are usually about twice as wide as they are long in the direction of the longitudinal body axis. They carry strong longitudinal ridges parallel to that axis, sometimes with intercalated thinner ones in between.

Hyoid arch: All specimens described here show remains of the hyoid arch, although mostly their ventral side. Since the skeletons were embedded on their backs, the ventral part is often not perfectly preserved. Laterally flattened remains of the ceratohyals can be seen in Figure 11A$_4$ (PIMUZ A/I 5752), but neither the anterior not the posterior ends are complete. They have an oval cross section and posteriorly, they curve dorsally and widen. The partial right ceratohyal is about 120 mm long. The ceratohyals and hyoids are rather fragmentary in B ESEFB-LTM-203 (Fig. 7A$_1$, A$_4$, A$_6$). In PIMUZ A/I 5753 (Fig. 5), a pair of elongate conical cartilages lie on the mesial side of the anterior end of the Meckel's cartilages. They are about 50 mm long and 10 mm wide, laterally flattened and taper anteriorly. Their symmetric appearance suggest that they are cartilages separate from the ceratohyals and thus likely hypohyals. The left hyoid is preserved in situ in PIMUZ A/I 5752. It is about 170 mm long, has a flat oval cross section, and runs dorsomesially of the left palatoquadrate. Posteriorly, the hyoid is covered by the palatoquadrate laterally and by sediment. The hyoid follows the posterodorsal arc of the palatoquadrate and becomes higher anteriorly, where it reaches a height of 41 mm (Fig. 12).

Branchial skeleton: The ventral part of the branchial basket of PIMUZ A/I 5751 is nearly completely preserved (Figs. 3, 12A$_3$), but only the ventral aspect is exposed, and the cartilages are strongly weathered. The left rami of the incomplete ceratohyal and the five, more or less complete, rod-shaped and grooved ceratobranchials are less weathered than those from the right side. The left ceratobranchials are about 200 mm long and 20 mm wide, but do not display further morphological detail. They are still in articulation with the basibranchial copula. The copula is a 290 mm long blade-like plate, which is about 70 mm wide anteriorly. It tapers posteriorly and displays two converging furrows on its venter. The anterior margin is missing. There might be fragments of hypobranchials but they are either very fragmentary or covered

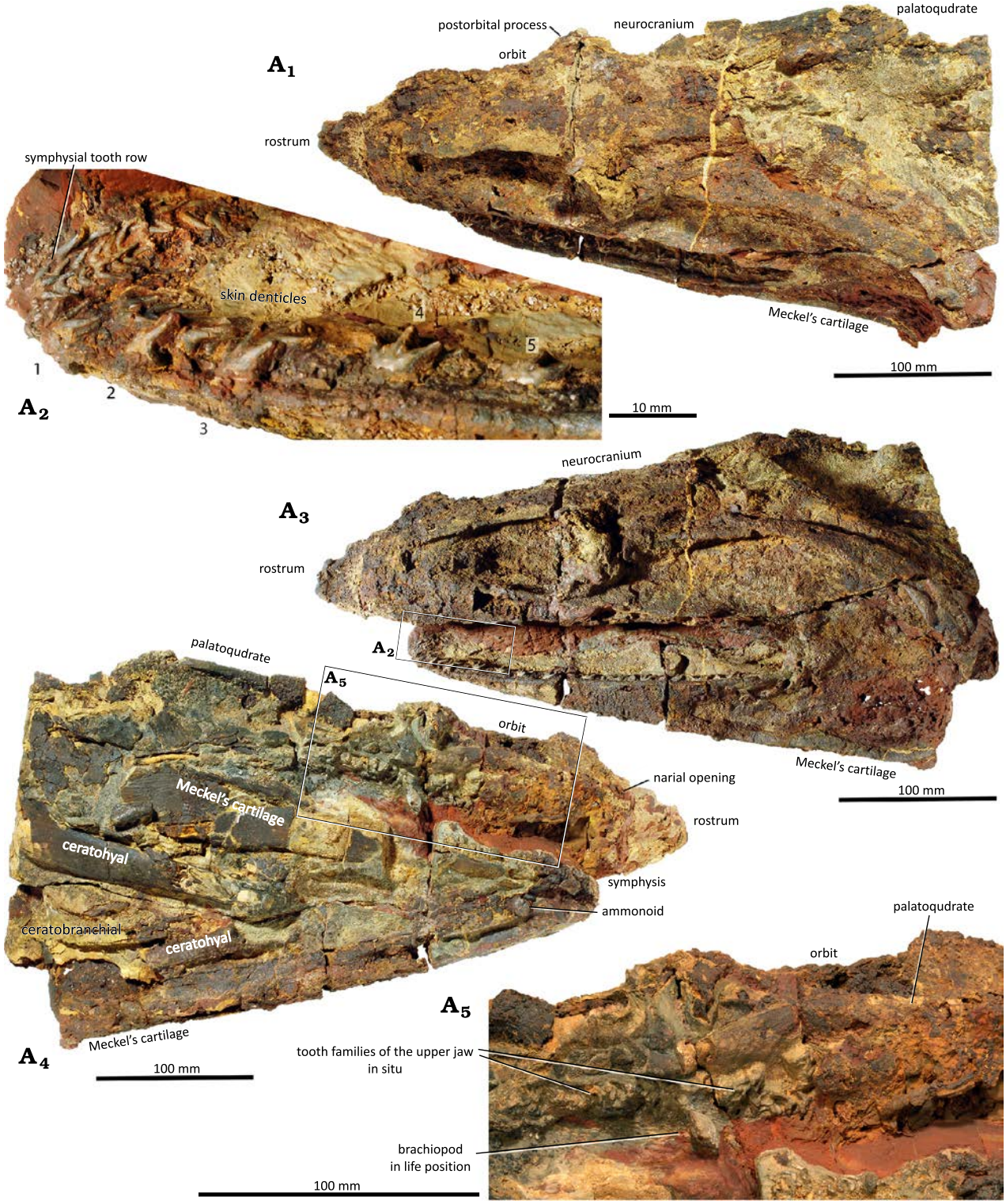

Fig. 11. Detail of the head of the phoebodontiform elasmobranch *Phoebodus saidselachus* Frey et al., 2019a (PIMUZ A/I 5752), middle Famennian, Upper Devonian, southern Maïder, Anti-Atlas, Morocco. Photographs of specimen in dorsolateral view (A_1), note that the teeth do not occupy the elevated margin of the outside of the Meckel's cartilage; detail of dentition of lower jaw; the symphyseal teeth are smaller and hardly change in size and shape through ontogeny (A_2); specimen in lateral (A_3) and oblique ventral (A_4) views; note the large ceratohyals and ceratobranchials in situ; detail showing the dentition and the brachiopod in life position (A_5).

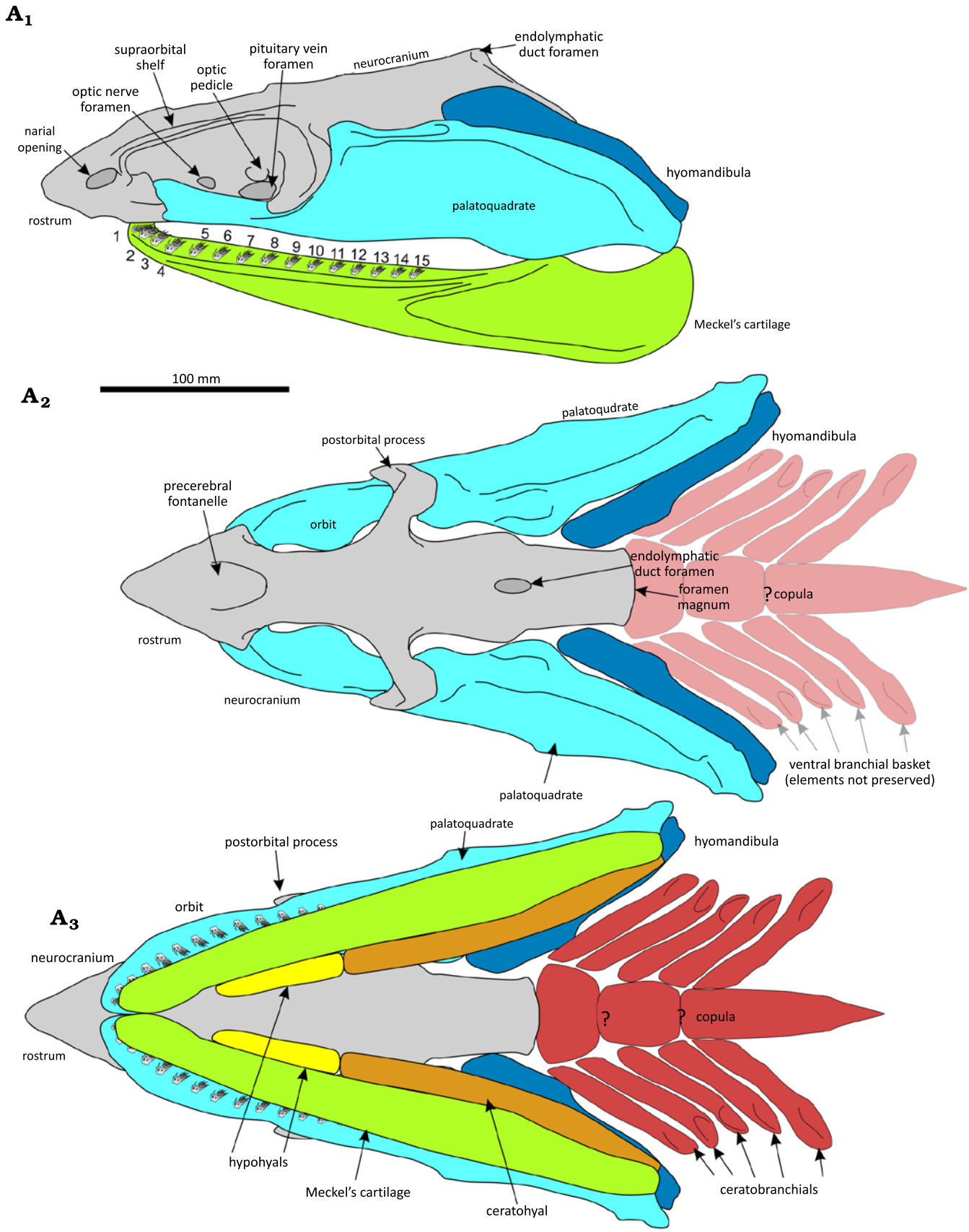

Fig. 12. Reconstruction of the head of the phoebodontiform elasmobranch *Phoebodus saidselachus* Frey et al., 2019a, middle Famennian, Upper Devonian, southern Maïder, Anti-Atlas, Morocco. Combining features of various specimens. Lateral (A_1), dorsal (A_2), and ventral (A_3) views. Grey, neurocranium; light blue, palatoquadrate; dark blue, hyoid; light green, Meckel's cartilage; orange, ceratohyal; red, branchial skeleton.

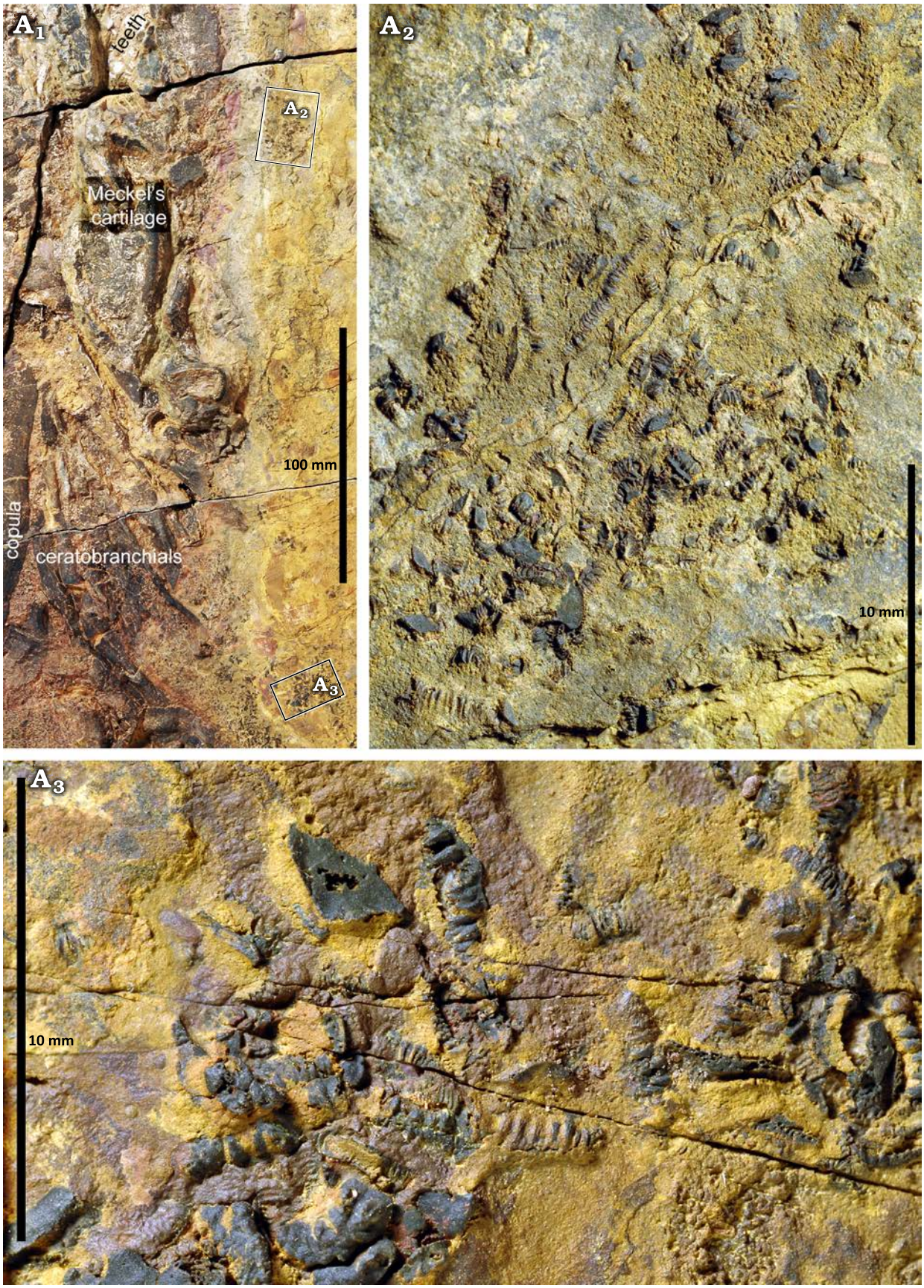

Fig. 13. The phoebodontiform elasmobranch *Phoebodus saidselachus* Frey et al., 2019a (PIMUZ A/I 5753), middle Famennian, Upper Devonian, southern Maïder, Anti-Atlas, Morocco. An overview of the head region (A_1), the denticles from the middle (A_2) and posterior (A_3) head region.

by the copula and ceratobranchials, because all specimens came to rest on their backs when they were embedded.

The copula of PIMUZ A/I 5753 (Fig. 5, 12A_3) is flat and teardrop-shaped with a pointed posterior end. It is about 170 mm long and 63 mm wide. Four pairs of ceratobranchials are still articulated but strongly crushed. They are 100 to 120 mm long, but in all cases, both ends are either covered or poorly preserved. Their width varies between 20 and 25 mm in their flattened state. Nevertheless, they display traces of a broad groove.

Neural arches: As in other early chondrichthyans, the neural arches vary morphologically from lower and longer shapes to slenderer and higher forms. While the anterior neural arches of PIMUZ A/I 5753 (Fig. 5) are about 17 mm long and 21 mm high, the neural arches posterior of the dorsal fin spine are up to 46 mm high and about 8 to 9 mm wide and dorsally pointed. There are about 13 of the low and broad neural arches exposed between the scapulocoracoids. Directly behind the fin spine is a group of 22 slender neural arches. On the most posterior patch of preserved integument, another 18 neural arches are discernible. While directly behind the fin spine, the arches appear to be aligned in a subparallel manner, all the posterior neural arches are chaotically arranged.

Dorsal fins: PIMUZ A/I 5752 has the best-preserved dorsal fin spines and fins. Although only preserved as external mould, the anterior dorsal fin spine displays the fine ornament of longitudinal ridges with pectinate crenulations (Figs. 14–16). It is about 220 mm long and 40 mm wide with a gently arched anterior and a subtly curved posterior edge. The apex is missing, probably it broke off before the animal deceased, because both sides of the external mould show that it was already incomplete when it was embedded. The posterior sulcus extends from the base to about 50 mm below the preserved part of the apex. The smooth shaft of the spine, which was inserted in the body, is about 90 mm long at the trailing edge. The ornamented part of the spine carries over 40 costae with either crescent-shaped pectinate tubercles or small conical spines on the posterior costae. We did not see any tubercles on the posterior edge below the apex. The angle of the lower end of the ornamented part is close to 40° and points at a rather low angle of insertion. This fin spine resembles *Ctenacanthus varians* St. John & Worthen, 1875 (see also Maisey 1981).

The basal cartilage measures about 170 mm in height and nearly 200 mm in length (Fig. 14). The dorsal fin was at least 150 mm long and high. It preserves the integument, which consists of vertical rows of polyodontode dermal denticles (growing scales; Reif 1982). These rows are about 1 mm wide. The limits between the denticles are difficult to identify, but it appears like the denticles were about 2 to 3 mm long in dorsoventral direction.

The fin spine of the posterior dorsal fin of PIMUZ A/I 5752 (Fig. 16A_2) is much thinner and slightly shorter than the anterior one. Its external mould is 135 mm long and up to 20 mm wide. The smooth shaft is about 55 mm long at the posterior edge. The ornament consists of about 18 finely ornamented costae. This fin spine closely resembles *Ctenacanthus denticulatus* McCoy, 1848 (Maisey 1981: fig. 8F, G) in its slenderness, fine pectinate costulation, and the low angle of insertion (supporting that this is a posterior fin spine). Fin cartilage and the fin are mostly weathered away.

PIMUZ A/I 5751 also preserves external moulds of both fin spines. The anterior fin spine is laterally compressed, 150 mm long and 63 mm wide at its base. It displays a fine longitudinal striation. The posterior fin spine is 208 mm long and up to 30 mm wide. It carries costae on its left side, which are crenulated and ramify from proximally. Around the posterior fin spine, shallow furrows might represent neural arches or radials of the dorsal fin. Only the 210 mm long and 30 mm wide fin spine of the anterior dorsal fin of PIMUZ A/I 5753 is preserved. It displays less of the pectinate costae than PIMUZ A/I 5752, but this may be due to the smaller size and earlier ontogenetic stage.

Pectoral girdle and fins: The scapulocoracoids are well preserved in PIMUZ A/I 5753 (Figs. 5, 17). They display an anteriorly convex coracoid region with a broad ventral-posterior concavity, ventral to the articular crest for the pectoral fin radials. The dorsal scapular part ends in a broad triangular structure with an acute anterior process and a blunt angled posterior process.

Anterior to the right scapulocoracoid, a heavily fragmented cartilage is preserved, which displays a concave articulation facet for the scapulocoracoid. Due to the overlap with other branchial cartilages, it is difficult to reconstruct its outline.

Both pectoral fins of PIMUZ A/I 5753 (Figs. 5, 17, 18) display their nearly complete cover of denticles, while only a few rectangular cartilages are preserved at the fin base. Similar cartilages lie between the scapulocoracoids and the copula. Thus, they may be rather the longitudinally stretched anterior neural arches than proximal radials of the pectoral fin. By contrast, these cartilages lie on the denticles instead of below, which is difficult to explain in both cases.

The polyodontode dermal denticles of PIMUZ A/I 5753 show some variation in size and shape within the pectoral fins (Fig. 18). They share flat rhomboid bases with the long axes running subparallel to the anterior edge of the fins. The largest denticles are found at the anterior edge of the fin (Fig. 18A_2, A_5), close to the trunk. They measure up to 5 × 2 mm and carry up to ten strong bulges on the crown with a rounded anterior side and a tapering trailing side. Both the anterior and the posterior edges display much finer ridges, possibly up to 20 per side in the largest denticles. Near the tip of the fin (Fig. 18A_1), the rhomboid denticles are maximum 1.5 mm wide and 0.5 to 0.8 mm long. Their crowns carry only four or five of the strong ridges. The denticles in the middle of the fin (Fig. 18A_3) measure 2 × 1 mm and have a similar shape.

Pelvic girdle: Only questionable remains of the pelvic fins are preserved in PIMUZ A/I 5751. Opposite of the posterior fin spines, two furrows are visible, which are 150 and

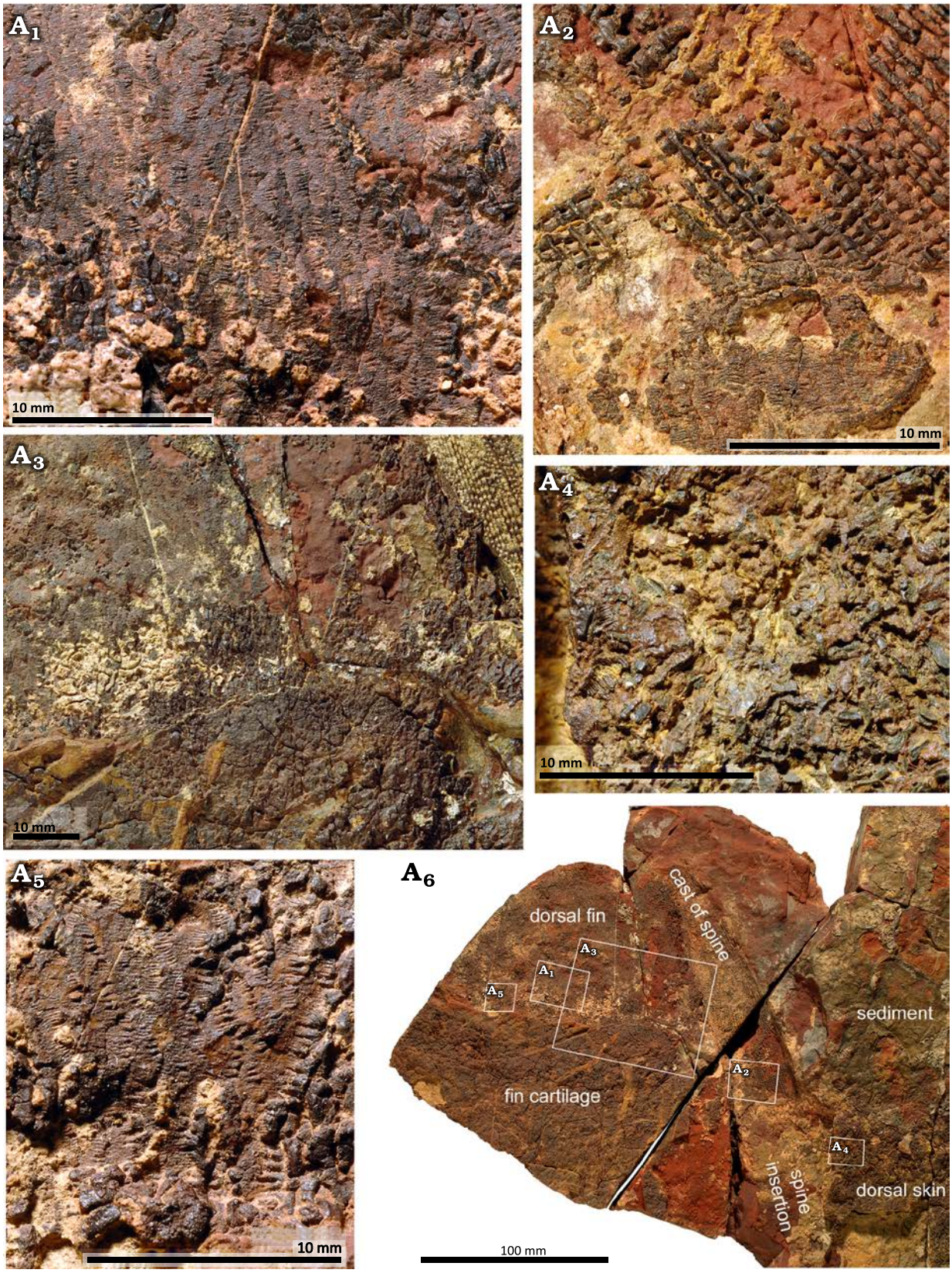

Fig. 14. Anterior dorsal fin of the phoebodontiform elasmobranch *Phoebodus saidselachus* Frey et al., 2019a (PIMUZ A/I 5751), middle Famennian, Upper Devonian, southern Maïder, Anti-Atlas, Morocco. Photographs showing general view of the specimen (A_6); dermal denticles in situ (A_1), note the fine striation of the polyodontode denticles, which likely served to reduce drag; base of ornamented part of fin spine (A_2), which was likely not covered by living tissue (at the bottom, the squamation of the dorsum is still preserved, documenting the deep insertion of the spine); detail showing basal cartilage and how it inserts posteriorly into the fin spine (cast) (A_3); slightly disarticulated skin of the dorsum anterior to the fin spine (A_4); enlarged detail of squamation on the fin (A_5).

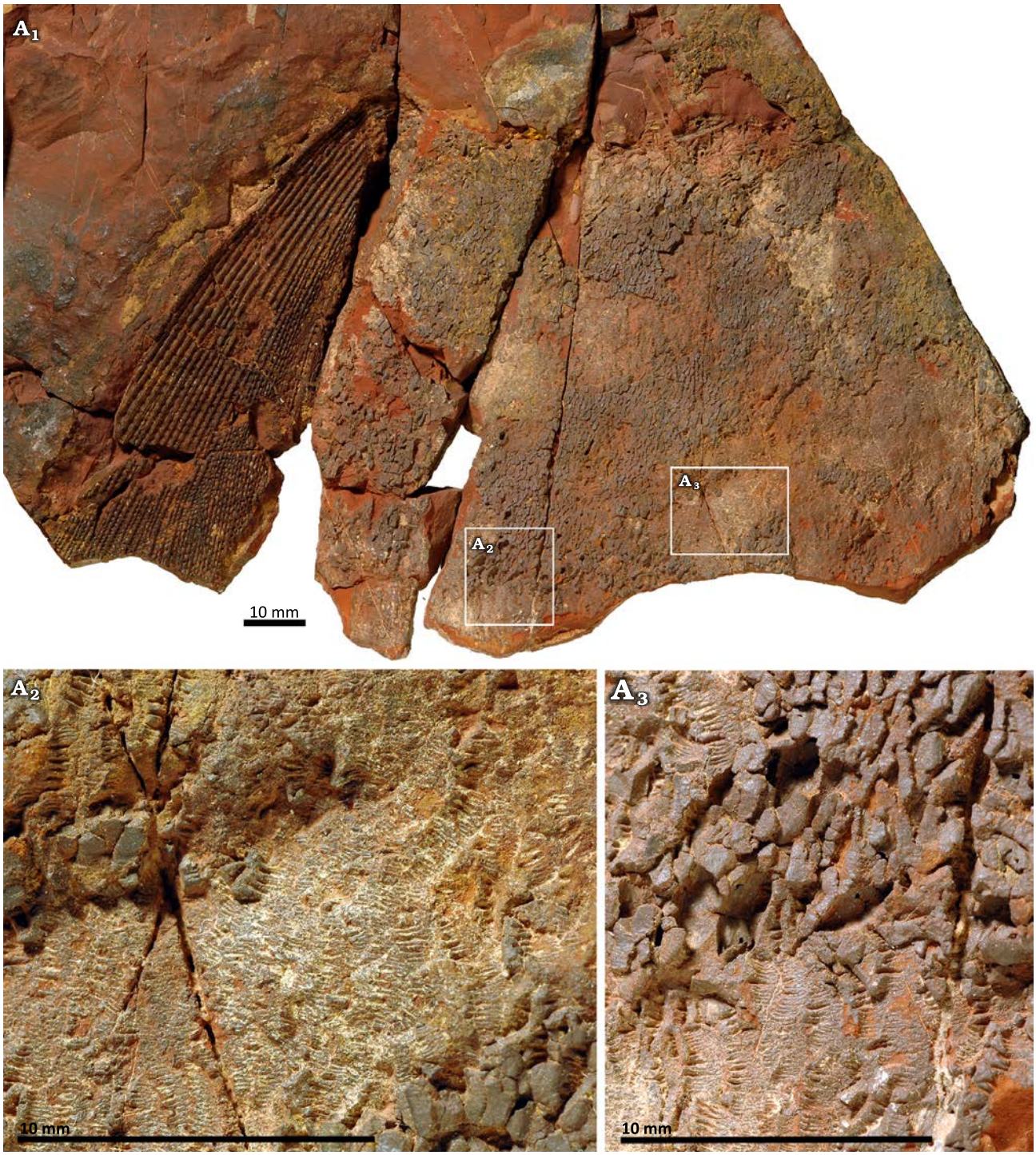

Fig. 15. Anterior dorsal fin of the phoebodontiform elasmobranch *Phoebodus saidselachus* Frey et al., 2019a (PIMUZ A/I 5751), middle Famennian, Upper Devonian, southern Maïder, Anti-Atlas, Morocco. Photographs showing fin and fin spine cast: general view of the specimen (A_1), detail of the articulated squamation (A_2), note the fine striation parallel to the long body axis for drag reduction and the long axes of the denticles running subparallel to the fin spine; detail showing both the outer surface and the bases of the denticles (A_3).

120 mm long (Fig. 3). They meet anteriorly at a nearly right angle. The left ramus of this structure is associated with a set of subparallel furrows diverging from it and turn posteriorly. About ten such furrows are discernible. Based on position, proportions and arrangement of these possible external moulds, we assume that these are weathered remains of the pelvic fins with the long rods representing the basipterygium and the finer rods being radials.

Caudal fin: Only the cartilages of the ventral lobe of the caudal fin are preserved in PIMUZ A/I 5751 (Fig. 3). There are remains of about twelve rays. The proximal radials are up to 70 mm long and between 6 and 9 mm wide, while the

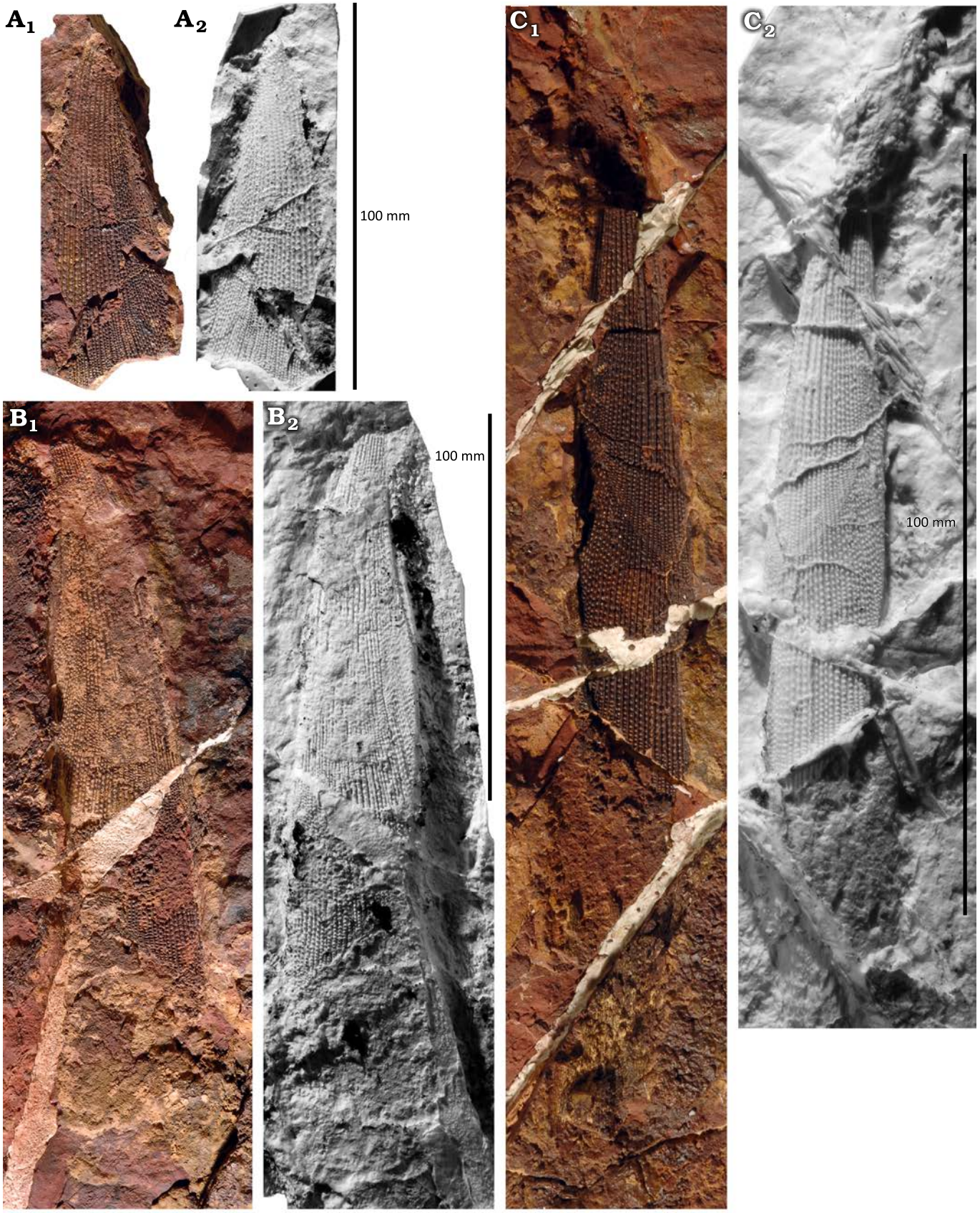

Fig. 16. Fin spines of the phoebodontiform elasmobranch *Phoebodus saidselachus* Frey et al., 2019a (PIMUZ A/I 5752), middle Famennian, Upper Devonian, southern Maïder, Anti-Atlas, Morocco. **A**, **B**. External moulds of left (**A**) and right (**B**) anterior fin spine; note the delicate ornament. **C**. External mould of posterior fin spine, note the fine striation and the growth irregularity in the middle of the spine. A_1 –C_1, photographs; A_2 –C_2, latex casts

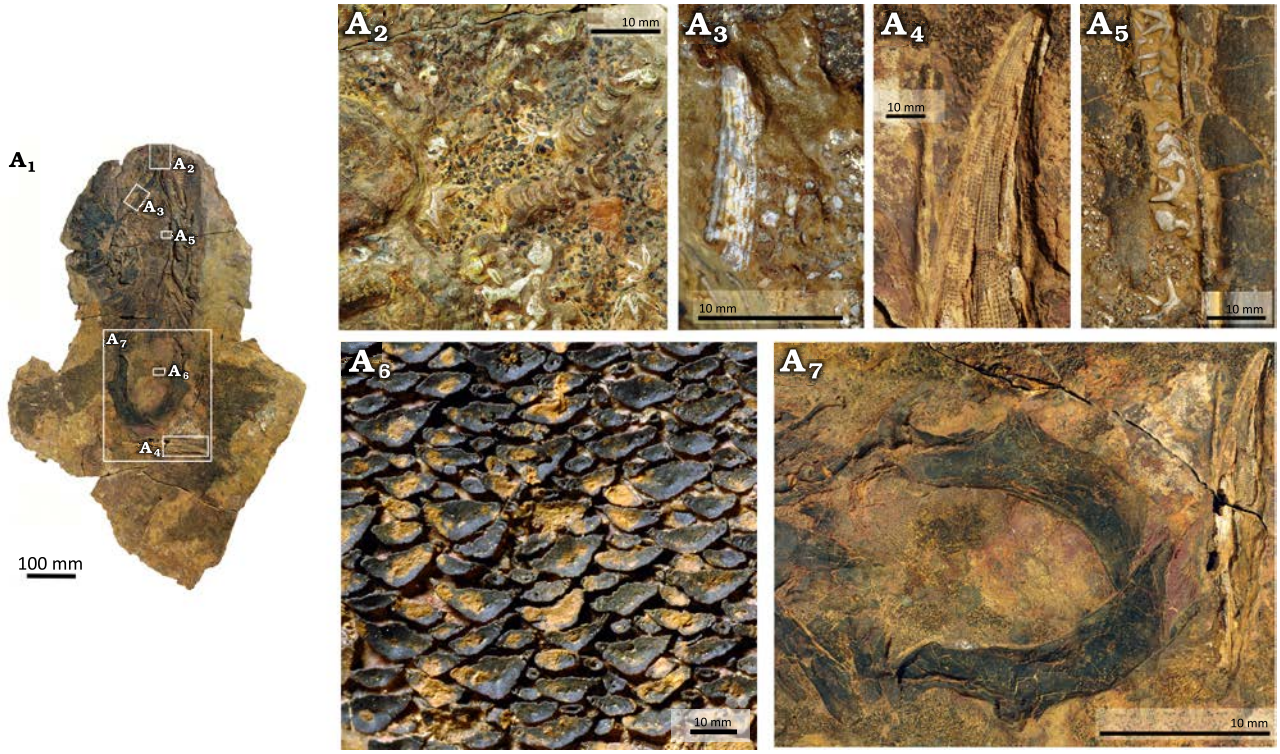

Fig. 17. Partial skeleton of *the phoebodontiform elasmobranch Phoebodus saidselachus* Frey et al., 2019a (PIMUZ A/I 5753), middle Famennian, Upper Devonian, southern Maïder, Anti-Atlas, Morocco. Specimen preserves skull and the pectoral region including skin: general view of the specimen (A_1), detail of symphyseal teeth, which expose the bases (A_2), fin spine of another chondrichthyan resembling, e.g., *Acondylacanthus*, which is stuck in the left posteroventral side of the ?neurocranium or palatoquadrate (A_3), detail of the anterior dorsal fin spine (A_4) some teeth between the jaws (A_5), bases of the skin denticles between the scapulocoracoids (A_6), scapulocoracoids, procoracoids, and the anterior dorsal fin spine (A_7).

distal radials are about 6 mm wide at the base and tapering distally. The most anterior distal radial is about 50 mm long while the longest measures 150 mm.

The caudal fin is the most important part of specimen PIMUZ A/I 5754, since it presents the only case where both lobes of the caudal fin are preserved, although only imperfectly articulated (Fig. 19A_3, A_4). We conclude that this is the fin of *Phoebodus saidselachus* because the neural arches of *Maghriboselache* are slenderer and more elongate than those preserved here, especially near the base of the dorsal lobe. There are remains of at least ten hypochordal radials, which are up to 66 mm long. They are still arranged nearly parallel to each other and as in PIMUZ A/I 5751, some of the rays display an articulation, while some contain only one cartilaginous element. The haemal spines are up to 35 mm long and lie roughly in a line, although in a slightly chaotic way with varying degrees of displacement. The neural spines are preserved nearly in their original order. About neural spines are discernible, displaying the slightly sinusoidal shape with a tip each pointing posterodorsally and anteroventrally. These neural spines are up to 18 mm long and vary a lot in sagittal length from about 10 mm anteriorly and 4 mm more posteriorly.

Stratigraphic and geographic range.—The Maider and Tafilalt regions in the eastern Anti-Atlas, Morocco; upper lower and middle Famennian.

Discussion

Tooth replacement.—Aside from the rather striking preservation of neurocranial morphology of *Phoebodus* with its stark contrast to the spade-headed contemporaneous *Maghriboselache,* the most interesting feature of *Phoebodus saidselachus* is that it provides the earliest strong evidence of the characteristic mode of tooth generation and a high rate of shedding. The exceptional preservation of PIMUZ A/I 5752 shows no evidence of retention of smaller, ontogenetically older teeth scattered around the gape. Successive teeth within each tooth family differ only slightly in size (Fig. 11A_2). Furthermore, all of the tooth sets are confined within the labial margin of the tooth-bearing parts of the Meckel's cartilages and the palatoquadrates.

We suggest that shedding rather than retention probably reflects an increased rate of tooth generation in *Phoebodus* (see also Greif et al. 2026). In the case of elevated rates of tooth generation, extra space for tooth retention would have been required. In contrast to other Palaeozoic chondrichthyans like, e.g., *Ctenacanthus* or *Dracopristis* (Hodnett et al. 2021; MG unpublished data), the jaws are much lower and slenderer, reducing space for tooth retention. Elevated rates of shedding and replacement might also suggest elevated functionality, with worn and blunt teeth replaced promptly, thereby increasing performance of the bite. As Greif et al.

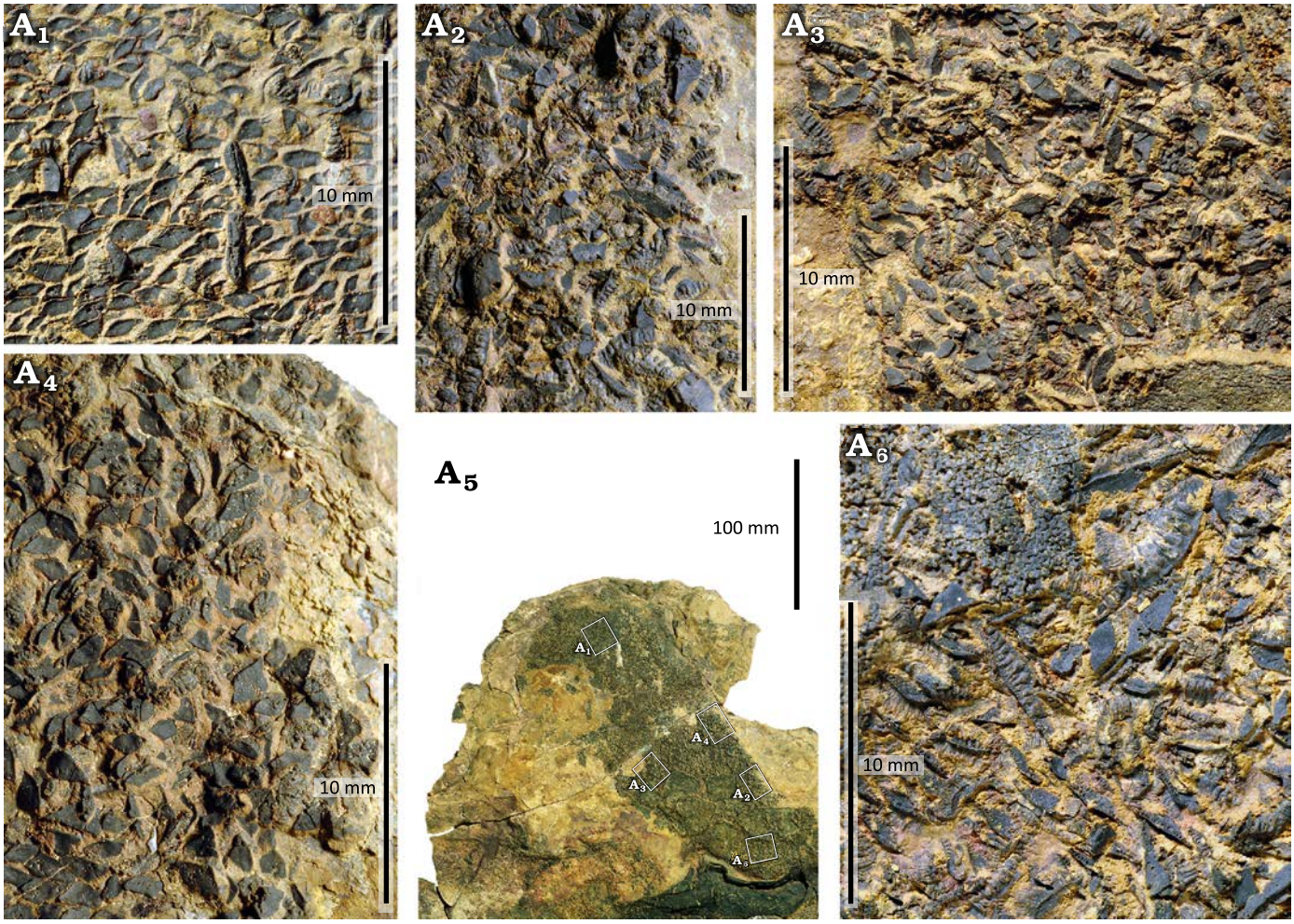

Fig. 18. Right pectoral fin of the phoebodontiform elasmobranch *Phoebodus saidselachus* Frey et al., 2019a (PIMUZ A/I 5753), middle Famennian, Upper Devonian, southern Maïder, Anti-Atlas, Morocco. General view of the specimen (A_5); detail showing dermal denticle bases from close to the tip of the fin in situ with fragmentary ceratotrichia (A_1); elongate striated denticles from the centre of the fin with drag-reducing ridges (A_2, A_3), denticles in A_2 are preserved closer to the body than A_3; slightly disarticulated denticles from the anterior edge (A_4), the smaller and sturdier fins were likely adapted to withstand mechanical stress; denticles close to the proximal anterior insertion of the fin (A_6), note their large size and great width.

(2025) demonstrated, the teeth of *Ctenacanthus* sometimes show strong wear. A high tooth replacement rate guarantees maximum functionality in particular for grasping and puncturing prey. Also, in the case of prey with a tough integument that would break or wear tooth tips, elevated tooth replacement rates would be a great benefit.

Prey and feeding.—Neither bromalites nor any food remains were recognized inside the digestive system. The only exception is a 15 mm long fin spine stuck in the jaw of PIMUZ A/I 5753 (Fig. 17A_3). This is evidence that *Phoebodus* was an active predator attacking prey of at least moderate size at its maximum known body size of about 2.5 m.

Due to great similarities in the dentition, slender skull, overall body form and body size, a comparison with the globally distributed modern neoselachian *Chlamydoselachus* is warranted. According to Ebert (2003), this neoselachian genus feeds on nudibranchs, smaller sharks (e.g., *Apristurus*), bony fish, and cephalopods including genera such as the decabrachians *Chiroteuthis*, *Histioteuthis*, *Onychoteuthis*, *Sthenoteuthis*, and *Todarodes* (Kubota et al. 1991). *Phoebodus* and *Chlamydoselachus* likely shared a rather weak bite because of the long Meckel's cartilages and the modes of articulation (far back). Kubota et al. (1991) found only little food in dissected frilled sharks, which suggests rapid digestion. In turn, this could explain the scarcity of preserved stomach contents although the skeletons preserve delicate features such as intact skin otherwise.

PIMUZ A/I 5754 is associated with a skeleton of *Maghriboselache*. The cartilages of both specimens are preserved on the same plane, making the assignment to either species impossible in several cases, leading to the assumption that they were really embedded together. The skeletal elements of both individuals are so mixed that we must assume that they died more or less simultaneously. Current alignment appears unlikely since one would expect that their long body axes would become aligned in parallel, which is not the case: the skeleton of *Phoebodus saidselachus* is undulating around the skull of *Maghriboselache*,

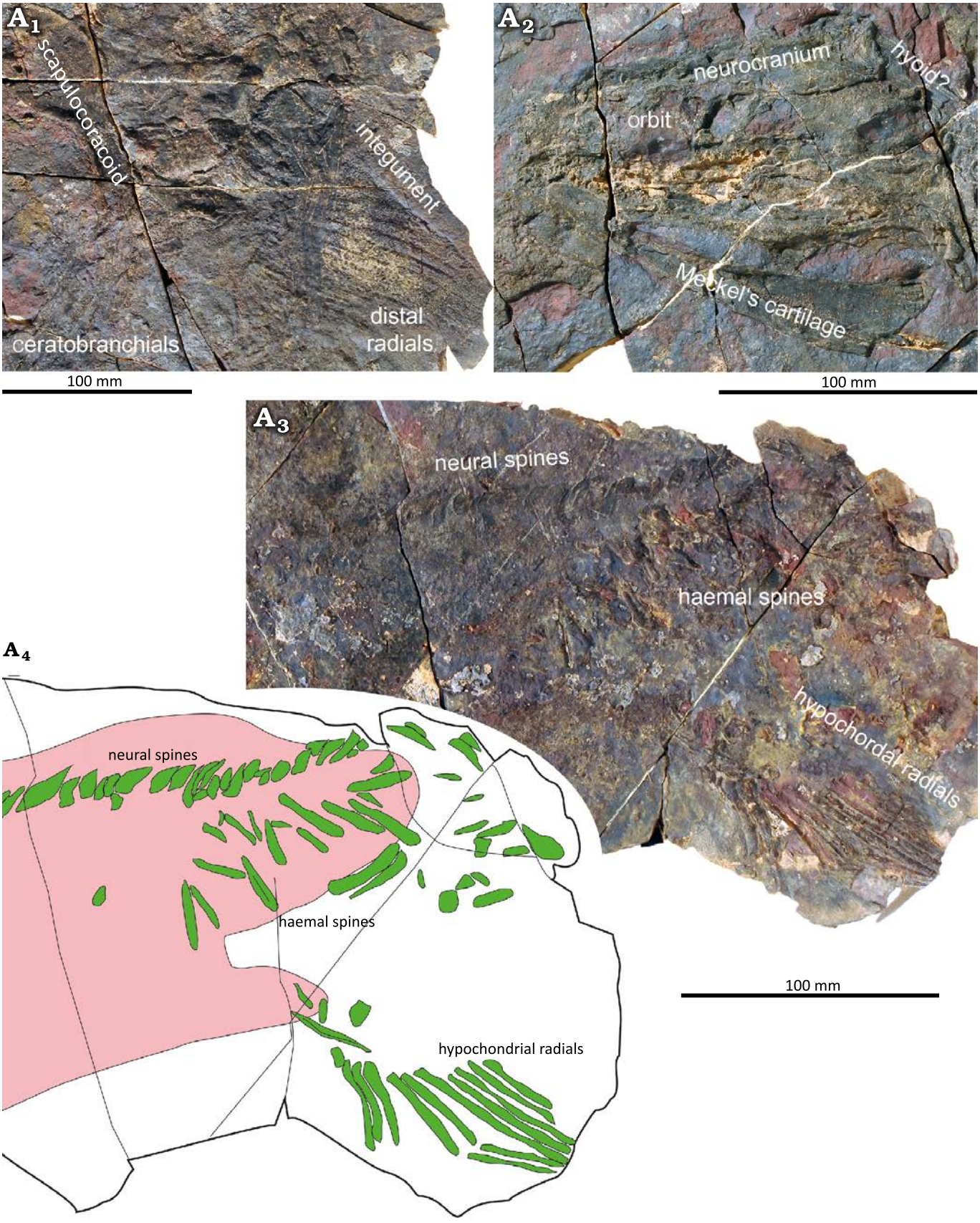

Fig. 19. The phoebodontiform elasmobranch *Phoebodus saidselachus* Frey et al., 2019a (PIMUZ A/I 5754), middle Famennian, Upper Devonian, southern Maïder, Anti-Atlas, Morocco. Pectoral fin and scapulocoracoid (A_1), note that it is not clear whether this pectoral region belongs to *Maghriboselache mohamezanei* or *Phoebodus saidselachus*; crushed head region (A_2); caudal fin (A_3, photograph; A_4, line drawing), much of the slab is covered with skin denticles.

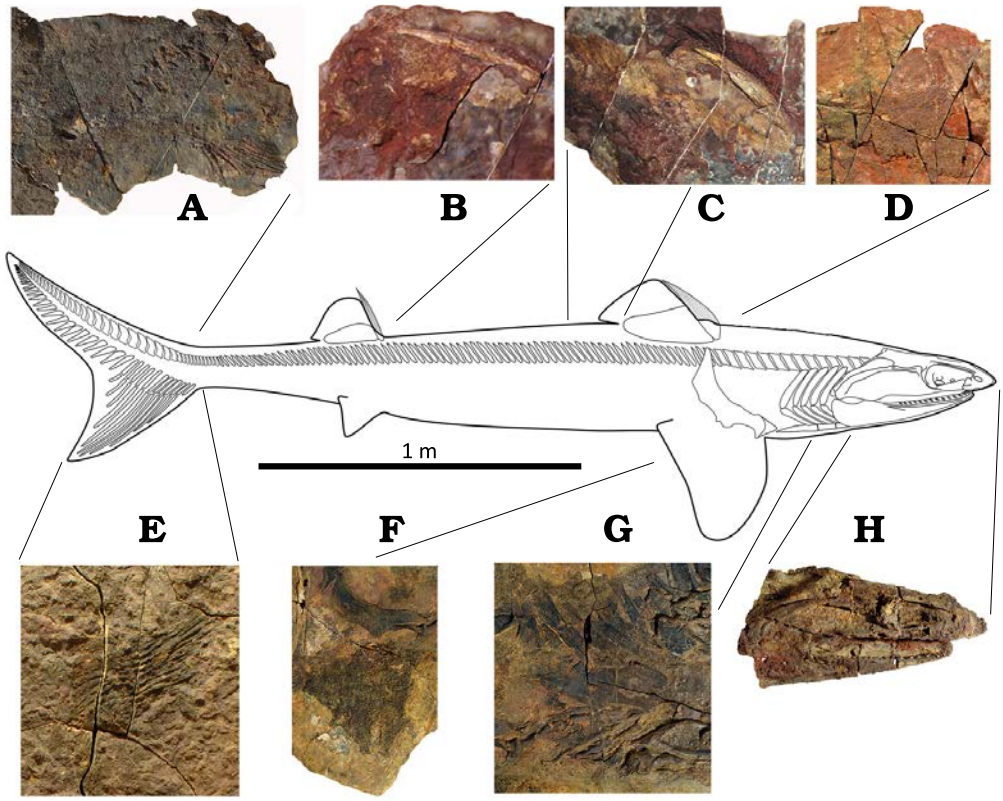

Fig. 20. Skeletal reconstruction of the phoebodontiform elasmobranch *Phoebodus saidselachus* Frey et al., 2019a, middle Famennian, Upper Devonian, southern Maïder, Anti-Atlas, Morocco. **A**. PIMUZ A/I 5754, caudalis. **B**, **C**. PIMUZ A/I 4712, posterior and anterior dorsal fins. **D**. PIMUZ A/I 5752, anterior dorsal fin. **E**. PIMUZ A/I 5751, caudalis. **F**, **G**. PIMUZ A/I 5753, pectoral fin and branchial basket. **H**. PIMUZ A/I 5752, head. The photos are not to scale. The scale refers only to the drawing.

while the latter looks like it is coiled up in the middle of the slab. Accordingly, we suggest a pre-mortem interaction, which possibly led to their demise. It is rather unlikely that either one attempted to prey on the other since their skulls are of similar dimensions. Territoriality is rare among modern chondrichthyans while agonism (behaviours related to conflicts between competing organisms) has been reported from 23 species (Baldridge and Williams 1969; Martin 2007). If these Devonian sharks were involved in some agonistic behaviour, it is likely that it was the intention of neither individual to kill the opponent since this involves great risks (Martin 2007), especially since they were of similar size and have similar grasping dentitions. If they interacted directly, then this could be another case of fossilized distraction sinking (Mapes et al. 2019; Klug et al. 2021), i.e., the two animals were so busy with their interaction that they sank into the oxygen-depleted bottom waters and suffocated together.

Indirect evidence for the diet of *Phoebodus* can be extracted from the dentition. The tricuspid teeth with their slender cusps can be considered a grasping dentition, suitable for holding prey such as, for example, smaller fish, conodonts or other animals with a slippery body (Cooper et al. 2023). Tooth wear played a lesser role, since the tooth replacement was likely higher than in other Devonian chondrichthyans such as *Ctenacanthus* (Greif et al. 2026), the co-occurring ammonoids were mostly of small size (< 50 mm conch diameter), and thus they could have been swallowed in their entirety. There are no teeth on the outer margin of the Meckel's cartilage as in *Ctenacanthus* (Greif et al. 2025) or *Symmorium* (ongoing research on own material by MG and CK).

Growth and size differences.—The sizes of the available skeletons range from about one metre (PIMUZ A/I 4712, the holotype) to about 2.5 m (PIMUZ A/I 5751 and A/I 5752). Although the body is not preserved three-dimensionally, the shape of the nodule and the proportions of the pectoral girdle as well as the relative positions of the fins provide a rough impression of the body shape (Figs. 20, 21).

Variation of both morphology and body size is influenced by many factors such as sex, environment (temperature, food availability etc.), illnesses, and injuries. Since we are not able to assign any of the specimens to either sex, we cannot rule out differences in size between the genders as in, e.g., the whale shark or the great white shark, where the females grow to bigger adult sizes.

Since the size differences between females and males in modern species are not in the range we found in the skeletons of *Phoebodus*, we exclude that it is only sexual dimorphism and can assume that age and thus growth stage explains size and shape differences at least to some degree. Accepting this, we suggest that juveniles up to around one

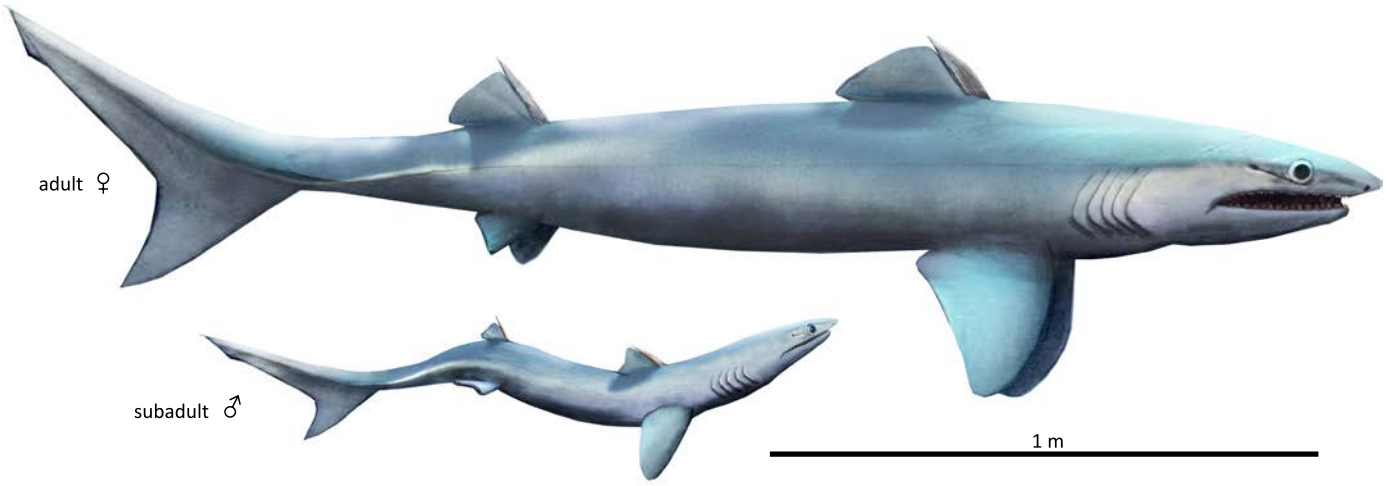

Fig. 21. Reconstructions of an adult female and juvenile male of the phoebodontiform elasmobranch *Phoebodus saidselachus* Frey et al., 2019a, middle Famennian, Upper Devonian, southern Maïder, Anti-Atlas, Morocco. We incorporated the new anatomical details particularly in the proportions and the fin shapes. The juvenile is reconstructed after the holotype.

metre length were still slenderer than supposed adults of over 2 m body length, which were still slender but much closer in shape to other Devonian chondrichthyans such as *Maghriboselache*. This increasing cross section-to-body length-ratio is not unusual in chondrichthyans and hence, we assume that this allometric change is to some degree growth-related. By contrast, the reconstruction provided by CK in Frey et al. (2019a: fig. 5a) is wrong in the missing ventral lobe of the caudal fin and the overly slim, anguiliform body shape. In turn, this enhances the contrast to the very eel-like Carboniferous *Thrinacodus* (Grogan and Lund 2008).

Phylogeny.—Frey et al. (2019a: fig. 4) recovered the genus *Phoebodus* as the earliest elasmobranch, where complete skeletons are known. This is consistent with published results from the Bayesian analysis of AP in Klug et al. (2023: fig. 13). With the new and previously unknown anatomical details provided here, we could better code *Phoebodus* and AP reran the analyses using the matrix produced by Coates et al. (2017) and modified by Frey et al (2019a) as well as Klug et al. (2023). For comparison, we used the matrix by Bronson et al. (2024).

Our new analyses produced somewhat contrasting results. The new scoring did not change the position of *Phoebodus* in the phylogeny in the stem of the elasmobranchs when using the character matrix of Coates et al. (2017), which was modified by Frey et al (2019a), Klug et al. (2023) as well as herein (Figs. 22, 23); independent of the used character matrix, the choice of taxa (Coates et al. 2017 versus Bronson et al. 2024), *Phoebodus* was placed in the elasmobranch stem in the Bayesian analyses, while in the parsimony analyses, *Phoebodus* was recovered in the chondrichthyan stem when using the Bronson matrix (Fig. 23B). While we interpret these results as pointing towards the placement of *Phoebodus* in the elasmobranch stem, we also highlight the need of a profound revision of the matrices, which is beyond the scope of this article.

The phoebodont clade is also rather close to the ctenacanthids, which likely gave rise to the xenacanthiforms, a group of chondrichthyans in the elasmobranch stem. With the phoebodontids, the members of this order share slender bodies, slender endocasts, and the teeth usually bearing two to three main slender cusps on a broad base. Xenacanthiforms differ from phoebodontids in their pseudo-diphycercal caudal fin (Soler-Gijón and Ruiz 2023), elongate dorsal fin, the presence of two anal fins, and a dorsal spine on the posterior of the neurocranium.

Possibly one of the most remarkable anatomical innovations that appeared with the phoebodontids are the slender and stream-lined body (quite extreme in *Thrinacodus/Thrinacoselache*) with a high caudal fin in *Phoebodus*, the elongated and pointed nose, which is reminiscent of modern pelagic sharks, and the likely rapid tooth replacement (Greif et al. 2026). These innovations characterize *Phoebodus* as the first shark displaying a series of traits that, in turn, characterize their modern elasmobranch relatives in contrast to, e.g., symmoriids or ctenacanthids (Greif et al. 2025).

Concerning the endocast, its overall shape is even slenderer than those of *Maghriboselache*, *Cladodoides*, and *Orthacanthus*. For example, the cerebellar region is slightly thickened in these genera and much thicker in derived symmoriids and crown holocephalans (e.g., Coates et al. 2017; Klug et al. 2023). Further, the small radius of the external semicircular canals are characteristic for vertebrates with a pelagic habit (Hullar 2006). All these characteristics are shared with many modern elasmobranch predators and mark *Phoebodus* as the first, fast swimming pelagic shark.

With the knowledge of the body proportions of *Phoebodus*, the difference to the very eel-like *Thrinacodus* (Grogan and Lund 2008) is even more extreme. We expect that Famennian representatives of *Thrinacodus* likely were

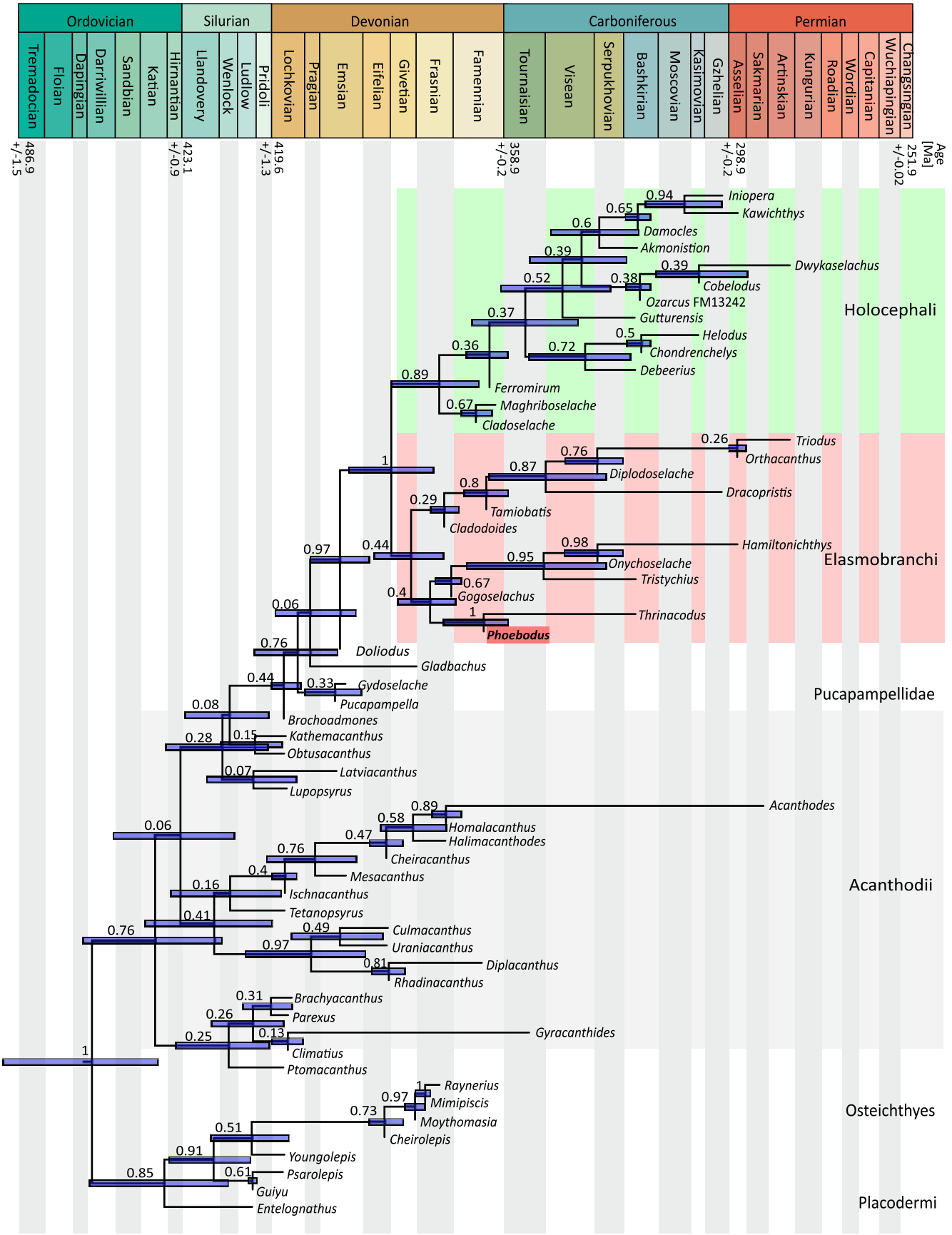

Fig. 22. Phylogeny based on the emended character matrix from Coates et al. (2017) and Frey et al. (2019a, 2020). Bayesian tip-dating analyses of 230 characters were performed using the fossilized birth–death model. Numbers shown at nodes represent posterior probabilities.

Fig. 23. Trees resulting from parsimony analyses, majority rule. **A**. Based on the emended character matrix of Coates et al. (2017) and Frey et al. (2019a, 2020). **B**. Based on the emended character matrix of Bronson et al. (2024). Numbers at the nodes indicate the frequency of occurrences of the respective node among the different trees.

morphologically intermediate between the species from Bear Gulch and *Phoebodus saidselachus*, i.e., the body was possibly slenderer than in *P. saidselachus* but less than in *Thrinacodus gracia*. Since teeth of *Thrinacodus* are moderately common in the Famennian of the Anti-Atlas, we expect that skeletal remains of this genus will be discovered sooner or later, shedding light on this question.

Conclusions

Newly prepared skeletons of the middle Famennian chondrichthyan *Phoebodus saidselachus* Frey et al., 2019a, provide a corrected anatomical picture of this important early elasmobranch. An undeformed skull was CT-scanned, and the image-stack yielded a model of the nearly complete neurocranium with endocast. The endocast displays several plesiomorphic aspects such as its slender form where neither the mesencephalon nor the cerebellar part is markedly inflated. The semicircular canals are very tightly packed lateral to the endocast and lengthened in sagittal direction, which is likely linked with the slender skull morphology and the open marine habitat.

Other skeletons display the dorsal fins with their ctenacanth-like fin spines. Especially the anterior dorsal fin is perfectly preserved including the large fin cartilage and the fin with the thick skin denticle cover. In both the anterior dorsal fin and the pectoral fins, the dermal cover consists of large rhomboid denticles with their long axes perpendicularly arranged to the long body axis. The denticles bear several strong folds running parallel to the body axis (main swimming direction). The heterocercal caudal fin is partially preserved in two specimens, displaying the elongated axial lobe and the high ventral lobe.

Overall, the body morphology suggests that *Phoebodus saidselachus* was a swift swimmer and efficient predator of small to moderately sized prey, since it had to swallow the prey in one piece. Moderately large, nektic prey is documented by the fin spine of another shark in the jaws of one specimen. Its numerous similarities to the neoselachian *Chlamydoselachus* (body form and size, tooth morphology and arrangement, slender skull shape, mandibular articulation point and jaw strength) is tentatively interpreted as being convergent, driven by similarities in the mode of life and properties of the diet. Comparing the shape of the skeletons depending on their size, it appears like the juveniles had more slender bodies than the adults, which were still rather slim animals, maybe comparable to, e.g., the blue shark *Prionace glauca*.

Acknowledgements

We wish to thank Ahmed Benlakhdim and his friendly team of the Ministère de l'Energie, des Mines, de l'Eau et de l'Environnement (Direction du Développement Minier, Division du Patrimoine, Rabat, Morocco) for providing working permits. All specimens were discovered and excavated by the great Saïd Oukharbouch (Tafraoute, Morocco). The material was professionally prepared by Thomas Imhof (Trimbach, Switzerland) and Rosemarie Roth (University of Zurich, Switzerland). Some of the photos were taken by Carlo Romano (University of Zurich, Switzerland). Bran Picozzi (University of Zurich, Switzerland) re-segmented the CT-image stack. Gabriel Aguirre Fernandez (University of Zurich, Switzerland) helped with the parsimony analyses. We also thank Hector Botella (University of Valencia, Spain) and an anonymous reviewer for thoroughly reading our manuscript versions and their equally detailed and constructive feedback. We greatly appreciate the financial support by the Swiss National Science Foundation SNF (project nr. 205320_215642).

Availability of data.—Supplementary material comprises ply-files of the neurocranium, endocast, and mandibular arch, a cropped image stack, the Mimics-file of the stack, the nexus-files used for the phylogeny, the RevBayes-output files and the two output files of the parsimony analyses and can be found in the SOM (Supplementary Online Material available at http://app.pan.pl/SOM/app71-Klug_etal_SOM.pdf). These files are available at Zenodo with the DOI 10.5281/zenodo.17533307.

Editor: Camila Cupello

References

Andreev, P.S., Sansom, I.J., Li, Q., Zhao, W., Wang, J., Wang, C.-C., Peng, L., Jia, L., Qiao, T., and Zhu, M. 2022. Spiny chondrichthyan from the lower Silurian of South China. *Nature* 609: 969–974.

Baldridge, H.D. and Williams, J. 1969. Shark attack: feeding or fighting? *Military Medicine* 134 (2): 130–133.

Barido-Sottani, J., Aguirre-Fernández, G., Hopkins, M.J., Stadler, T., and Warnock, R. 2019. Ignoring stratigraphic age uncertainty leads to erroneous estimates of species divergence times under the fossilized birth-death process. *Proceedings of the Royal Society B: Biological Sciences* 286: 20190685.

Bonaparte, C.L.J.L. 1838. *Iconografia della fauna italica per le quatro classi degli animali vertebrati. Tomo III: Pesci.* 266 pp. Salviucci, Roma.

Botella, H. 2006. The oldest fossil evidence of a dental lamina in sharks. *Journal of Vertebrate Paleontology* 4: 1002–1003.

Botella, H., Valenzuela-Ríos, J.I., and Martínez-Pérez, C. 2009. Tooth replacement rates in early chondrichthyans: a qualitative approach. *Lethaia* 42: 365–376.

Brazeau, M.D. 2009. The braincase and jaws of a Devonian 'acanthodian' and modern gnathostome origins. *Nature* 457: 305–308.

Brazeau, M.D. and Friedman, M. 2014. The characters of Palaeozoic jawed vertebrates. *Zoological Jounal of the Linnean Society* 170: 779–821.

Bronson A.W., Pradel A., Denton J.S.S., and Maisey J.G. 2024. A new operculate symmoriiform chondrichthyan from the Late Mississippian Fayetteville Shale (Arkansas, United States). *Geodiversitas* 46 (4): 101–117.

Carr, R.K. and Jackson, G.J. 2008. The vertebrate fauna of the Cleveland Member (Famennian) of the Ohio Shale. *In*: Guide to the Geology and Paleontology of the Cleveland Member of the Ohio Shale. 68th Annual Meeting of the Society of Vertebrate Paleontology, Cleveland, Ohio, October 15–18, 2008. *Ohio Geological Survey Guidebook* 22: 1–17.

Coates, M.I., Finarelli, J.A., Sansom, I.J., Andreev, P.S., Criswell, K.E., Tietjen, K., Rivers, M.L., and La Riviere, P.J. 2018. An early chondrichthyan and the evolutionary assembly of a shark body plan. *Proceedings of the Royal Society B* 285: 20172418.

Coates, M.I., Gess, R.W., Finarelli, J.A., Criswell, K.E., and Tietjen, K. 2017. A symmoriiform chondrichthyan braincase and the origin of chimaeroid fishes. *Nature* 541: 208–211.

Cooper, J.A., Griffin, J.N., Kindlimann, R., and Pimiento, C. 2023. Are shark teeth proxies for functional traits? A framework to infer ecology from the fossil record. *Journal of Fish Biology* 103: 798–814.

Derycke, C. 1992. Microrestes de sélaciens et autres vertébrés du Dévonien supérieur du Maroc. *Bulletin de Musée national d'Histoire naturelle* 14: 15–61.

Ebert, D.A. 2003. *Sharks, Rays, and Chimaeras of California*. 284 pp. University of California Press, Berkeley.

Frey, L., Coates, M., Ginter, M., Hairapetian, V., Rücklin, M., Jerjen, I., and Klug, C. 2019a. The early elasmobranch *Phoebodus*: phylogenetic relationships, ecomorphology, and a new time-scale for shark evolution. *Proceedings of the Royal Society B* 286: 20191336.

Frey, L., Coates, M.I., Tietjen, K., Rücklin, M., and Klug, C. 2020. A new symmoriiform from the Late Devonian of Morocco: novel jaw function in ancient sharks. *Communications Biology* 3 (681): 1–10.

Frey, L., Pohle, A., Rücklin, M., and Klug, C. 2019b. Fossil-Lagerstätten and preservation of vertebrates and invertebrates from the Devonian of Morocco (eastern Anti-Atlas). *Lethaia* 53: 242–266.

Gavryushkina, A., Welch, D., Stadler, T., and Drummond, A.J. 2014. Bayesian inference of sampled ancestor trees for epidemiology and fossil calibration. *PLoS Computational Biology* 10 (12): e1003919.

Ginter, M. and Maisey, J.G. 2007. The braincase and jaws of *Cladodus* from the Lower Carboniferous of Scotland. *Palaeontology* 50: 305–322.

Ginter, M., Hairapetian, V., and Klug, C. 2002. Famennian chondrichthyans from the shelves of North Gondwana. *Acta Geologica Polonica* 52: 169–215.

Ginter, M., Hampe, O., and Duffin, C.J. 2010. *Handbook of Paleoichthyology: Teeth*. 168 pp. Verlag Dr. Friedrich Pfeil, München.

Goloboff, P.A. and Morales, M.E. 2023. TNT version 1.6, with a graphical interface for MacOS and Linux, including new routines in parallel. *Cladistics* 39 (2): 144–153.

Greif, M., Botella, H., Scheyer, T., and Klug, C. 2026. Diversity of tooth mineralization patterns at the base of crown chondrichthyans. *Communications Biology* 56: 1–14.

Greif, M., Calandra, I., Lautenschlager, S., Kaiser, T., Mezane, M., and Klug, C. 2025. Reconstruction of feeding behaviour and diet in Devonian ctenacanth chondrichthyans using Dental Microwear Texture and Finite Element analyses. *Royal Society Open Science* 12: 240936: 1–22.

Greif, M., Ferron, H.G., and Klug, C. 2022. A minute Meckel's cartilage from the Devonian Hangenberg black shale in Morocco and its position in chondrichthyan jaw morphospace. *PeerJ* 10: e14418.

Grogan, E.D. and Lund, R. 2008. A basal elasmobranch, *Thrinacoselache gracia* n. gen and sp., (Thrinacodontidae, new family) from the Bear Gulch Limestone, Serpukhovian of Montana, USA. *Journal of Vertebrate Paleontology* 28: 970–988.

Heath, T.A., Huelsenbeck, J.P., and Stadler, T. 2014. The fossilized birth-death process for coherent calibration of divergence-time estimates. *Proceedings of the National Academy of Sciences* 111 (29): E2957-E2966.

Hodnett, J.-P.M., Grogan, E.D., Lund, R., Lucas, S.G., Suazo, T., Elliott, D.K., and Pruitt, J. 2021. Ctenacanthiform sharks from the Late Pennsylvanian (Missourian) Tinajas member of the Atrasado Formation, central New Mexico. *New Mexico Museum of Natural History and Science Bulletin* 84: 391–424.

Höhna, S., Landis, M.J., Heath, T.A., Boussau, B., Lartillot, N., Moore, B.R., Huelsenbeck, J.P., and Ronquist, F. 2016. RevBayes: Bayesian phylogenetic inference using graphical models and an interactive model-specification language. *Systematic Biology* 65: 726–736.

Hotton, N. 1952. Jaws and teeth of American xenacanth sharks. *Journal of Paleontology* 26: 489–500.

Hullar, T.A. 2006. Semicircular canal geometry, afferent sensitivity and animal behavior. *The Anatomical Record* 288: 466–472.

Huxley, T. 1880. *A Manual of the Anatomy of Vertebrated Animals*. 431 pp. D. Appleton and Co., New York.

Irisarri, I., Baurain, D., Brinkmann, H., Delsuc, F., Sire, J.-Y., Kupfer, A., Petersen, J., Jarek, M., Meyer, A., Vences, M., and Philippe, H. 2017. Phylotranscriptomic consolidation of the jawed vertebrate timetree. *Nature Ecology & Evolution* 1 (9): 1370–1378.

Janvier, P. 1996. *Early Vertebrates*. 393 pp. Oxford University Press, Oxford.

Jobbins, M., Haug, C., and Klug, C. 2020. Famennian thylacocephalans from Morocco and their role in Late Devonian foodwebs. *Scientific Reports* 10: 5129.

Kaufmann, B. 1998. Facies, stratigraphy and diagenesis of Middle Devonian reef- and mud-mounds in the Mader (eastern Anti-Atlas, Morocco). *Acta Palaeontologica Polonica* 48: 43–106.

Khakurel, B., Grigsby, C., Tran, T.D., Zariwala, J., Höhna, S., and Wright, A.M. 2024. The fundamental role of character coding in bayesian morphological phylogenetics. *Systematic Biology* 73: 861–871.

Klug, C., Coates, M.I., Frey, L., Greif, M., Jobbins, M., Pohle, A., Lagnaoui, A., Bel Haouz, W., and Ginter, M. 2023. Broad snouted cladoselachian with sensory specialisation at the base of modern chondrichthyans. *Swiss Journal of Palaeontology* 142 (2): 1–28.

Klug, C., Frey, L., Pohle, A., De Baets, K., and Korn, D. 2017. Palaeozoic evolution of animal mouthparts. *Bulletin of Geosciences* 92 (4): 511–524.

Klug, C., Kröger, B., Kiessling, W., Mullins, G.L., Servais, T., Frýda, J., Korn, D., and Turner, S. 2010. The Devonian nekton revolution. *Lethaia* 43: 465–477.

Klug, C., Schweigert, G., De Baets, K., and Fuchs, D. 2021. Distraction sinking and fossilized coleoid predatory behaviour from the German Early Jurassic. *Swiss Journal of Palaeontology* 140 (7): 1–12.

Kocsis, A.T. and Scotese, C.R. 2020. Mapping paleocoastlines and continental flooding during the Phanerozoic. *Earth-Science Reviews* 213: 103463.

Kubota, T., Shiobara, Y., and Kubodera, T. 1991. Food habits of the frilled shark *Chlamydoselachus anguineus* collected from Suruga Bay, central Japan. *Nippon Suisan Gakkaishi* 57 (1): 15–20.

Lebedev, O.A., Ivanov, A.O., and Linkevich, V.V. 2020. Chondrichthyan spines from the Famennian (Upper Devonian) of Russia. *Acta Geologica Polonica* 70: 339–362.

Lewis, P.O. 2001. A likelihood approach to estimating phylogeny from discrete morphological character data. *Systematic Biology* 50: 913–925.

Li, Q., Zhu, Y., Lu, J., Chen, Y., Wang, J., Peng, L. Wei, G., and Zhu, M. 2021. A new Silurian fish close to the common ancestor of modern gnathostomes. *Current Biology* 31: 1–8.

Long, J.A. and Trinajstic, K.M. 2018. A review of recent discoveries of exceptionally preserved fossil fishes from the Gogo sites (Late Devonian, Western Australia). *Earth and Environmental Science Transactions of the Royal Society of Edinburgh* 108: 1–7.

Maisey, J.G. 2005. Braincase of the Upper Devonian shark *Cladodoides wildungensis* (Chondrichthyes, Elasmobranchii), with observations on the braincase in early chondrichthyans. *Bulletin American Museum of Natural History* 288: 1–103.

Maisey, J.G. 1981. Studies on the Paleozoic selachian genus *Ctenacanthus* Agassiz. Part 1. Historical review and revised diagnosis of *Ctenacanthus*, with a list of referred taxa. *Novitates* 2718: 1–22.

Mapes, R.H., Landman, N.H., and Klug, C. 2019. Caught in the act? Distraction sinking in ammonoid cephalopods. *Swiss Journal of Palaeontology* 138 (1): 141–149.

Martin, R.A. 2007. A review of shark agonistic displays: comparison of display features and implications for shark–human interactions. *Marine and Freshwater Behaviour and Physiology* 40: 3–34.

Miyashita, T., Janvier, P., Tietjen, K., Berenguer, F., Schöder, S., Marone, F., Gueriau, P., and Coates, M.I. 2025. Novel assembly of a head–trunk interface in the sister group of jawed vertebrates. *Nature* 645: 686–691.

Mulvey, L.P.A., May, M.R., Brown, J.M., Höhna, S., Wright, A.M., and Warnock, R.C.M. 2025. Assessing the adequacy of morphological models using posterior predictive simulations. *Systematic Biology* 74 (1): 34–52.

Rambaut, A., Drummond, A.J., Xie, D., Baele, G., and Suchard, M.A. 2018. Posterior summarization in Bayesian phylogenetics using Tracer 1.7. *Systematic Biology* 67 (5): 901–904.

Reif, W.-E. 1978. Evolution of dermal skeleton and dentition in vertebrates. *Evolutionary Biology* 15: 287–368.

Sallan, L.C. and Coates, M.I. 2010. End-Devonian extinction and a bottleneck in the early evolution of modern jawed vertebrates. *PNAS* 107: 10131–10135.

Schaeffer, B. 1981. The xenacanth shark neurocranium, with comments on elasmobranch monophyly. *Bulletin of the American Museum of Natural History* 169: 1–66.

Schnetz, L., Butler, R.J., Coates, M.I., and Sansom, I.J. 2022. Skeletal and soft tissue completeness of the acanthodian fossil record. *Palaeontology* 65: e12616.

Schnetz, L., Butler, R.J., Coates, M.I., and Sansom, I.J. 2024. The skeletal completeness of the Palaeozoic chondrichthyan fossil record. *Royal Society Open Science* 11: 231451.

Schultze, H.-P. and Cloutier, R. (eds.) 1996. *Devonian Fishes and Plants of Miguasha (Canada)*. 374 pp. Verlag Dr. Friedrich Pfeil, München.

Simakov, O., Marlétaz, F., Yue, J.-X., O'Connell, B., Jenkins, J., Brandt, A., Calef, R., Tung, C.-H., Huang, T.-K., Schmutz, J., Satoh, N., Yu, J.-K., Putnam, N.H., Green, R.E., and Rokhsar, D.S. 2020. Deeply conserved synteny resolves early events in vertebrate evolution. *Nature Ecology & Evolution* 4 (6): 820–830.

Soler-Gijón, R. and Ruiz, A. D. 2023. "Carbonífero de Puertollano" Natural Monument (Puertollano basin, Spain): a window for the knowledge of Early Vertebrates. *Spanish Journal of Palaeontology* 38 (1): 81–94.

St. John, O. and Worthen A.H. 1875. Description of fossil fishes. *Geological Survey of Illinois* 6: 245–488.

Stadler, T. 2010. Sampling-through-time in birth-death trees. *Journal of Theoretical Biology* 267: 396–404.

Williams, M.E. 2001. Tooth retention in cladodont sharks: with a comparison between primitive grasping and swallowing, and modern cutting and gouging feeding mechanisms. *Journal of Vertebrate Paleontology* 21: 214–226.

Yang, Z. 1994. Maximum likelihood phylogenetic estimation from DNA sequences with variable rates over sites: Approximate methods. *Journal of Molecular Evolution* 39: 306–314.

Zhu, M., Zhao, W., Jia, L., Lu, L., Qiao, T., and Qu, Q. 2009. The oldest articulated osteichthyan reveals mosaic gnathostome characters. *Nature* 458: 469–474.

Zhu, M., Yu, X., Ahlberg, P.E., Choo, B., Lu, J., Qiao, T., Qu, Q., Zhao, W., Jia, L., Blom, H., and Zhu, Y. 2013. A Silurian placoderm with osteichthyan-like marginal jaw bones. *Nature* 502: 188–193.

Zhu, Y., Giles, S., Young, G.C., Hu, Y., Bazzi, M., Ahlberg, P.E., Zhu, M., and Lu, J. 2021. Endocast and bony labyrinth of a Devonian "Placoderm" challenges stem gnathostome phylogeny. *Current Biology* 31: 1–7.

Zhu, Y., Li, Q., Lu, J., Chen, Y., Wang, J., Gai, Z., Zhao, W., Yu, Y., Ahlberg, P., and Zhu, M. 2022. The oldest complete jawed vertebrates from the early Silurian of China. *Nature* 609: 954–958.